

RESEARCH ARTICLE

Plasmodium falciparum GCN5 acetyltransferase follows a novel proteolytic processing pathway that is essential for its function

Krishanu Bhowmick¹, Ankita Tehlan¹, Sunita², Renu Sudhakar³, Inderjeet Kaur⁴, Puran Singh Sijwali³, Annangarachari Krishnamachari² and Suman Kumar Dhar^{1,*}

ABSTRACT

The pathogenesis of human malarial parasite *Plasmodium falciparum* is interlinked with its timely control of gene expression during its complex life cycle. In this organism, gene expression is partially controlled through epigenetic mechanisms, the regulation of which is, hence, of paramount importance to the parasite. The *P. falciparum* (Pf)-GCN5 histone acetyltransferase (HAT), an essential enzyme, acetylates histone 3 and regulates global gene expression in the parasite. Here, we show the existence of a novel proteolytic processing for PfGCN5 that is crucial for its activity *in vivo*. We find that a cysteine protease-like enzyme is required for the processing of PfGCN5 protein. Immunofluorescence and immuno-electron microscopy analysis suggest that the processing event occurs in the vicinity of the digestive vacuole of the parasite following its trafficking through the classical ER-Golgi secretory pathway, before it subsequently reaches the nucleus. Furthermore, blocking of PfGCN5 processing leads to the concomitant reduction of its occupancy at the gene promoters and a reduced H3K9 acetylation level at these promoters, highlighting the important correlation between the processing event and PfGCN5 activity. Altogether, our study reveals a unique processing event for a nuclear protein PfGCN5 with unforeseen role of a food vacuolar cysteine protease. This leads to a possibility of the development of new antimalarials against these targets.

This article has an associated First Person interview with the first author of the paper.

KEY WORDS: Malaria, *Plasmodium falciparum*, GCN5, Histone acetyltransferase, Histone acetylation, Cysteine protease, Protein processing, ChIP sequencing, ChIP seq

INTRODUCTION

Epigenetics is one centrally important mechanism that determines how, where and when different genes are expressed and repressed. Reversible lysine acetylation of proteins is one of the major epigenetic modifications that have regulatory roles in diverse cellular functions. This crucial acetylation function is carried out by a class of proteins called histone acetyltransferases (HATs). Over the past decade, they have been implicated in fundamental biological processes and etiology of several diseases, such as


cancer, cardiovascular diseases and protozoan diseases (Croken et al., 2012; Trisciuglio et al., 2018; Wang et al., 2014). The mosquito-borne parasitic disease malaria is one of the ancient diseases persisting on earth, and still remains the most fatal parasitic disease on the planet. The protozoan parasite *Plasmodium* is the etiological agent for malaria; it infects ~219 million people each year and causes ~435,000 deaths annually (Barber et al., 2017). Among the five *Plasmodium* species, *Plasmodium falciparum* is responsible for the majority of the mortality and morbidity due to its ability to cause the most severe form of malaria. Despite ongoing efforts on global malaria control, progress has been stalled due to the continuous emergence of antimalarial-resistant parasites and lack of development of new therapeutics to combat this problem.

The histone acetyltransferase GCN5 was first identified as a stress response protein in yeast (Skvirsky et al., 1986). GCN5 is one of the best studied HATs, and GCN5s have been implicated in various cellular functions including acetylation of histone and non-histone proteins, transcription regulation, cell cycle control, early embryonic development, and B cell and T cell activation under certain conditions (Carrozza et al., 2003; Gao et al., 2017; Kikuchi et al., 2011; Phan et al., 2005). The principal substrates of GCN5 acetyltransferases are the N-terminal lysine residues of histone H3 (the lysine residues at positions 9, 14, 18, 23 and 56) (Grant et al., 1999; Smith et al., 1998; Xu et al., 1998). The acetylation of histone H3 at lysine 9 (H3K9Ac) is a major histone mark that is predominantly found on active gene promoters and is responsible for active gene transcription (Cui et al., 2007; Pokholok et al., 2005; Wang et al., 2008; Zhou et al., 2010). A role for the H3K9Ac histone mark beyond transcription activation has been reported recently. In mammalian cells, H3K9Ac directly recruits the super elongation complex (SEC) to the chromatin and triggers a switch from transcription initiation to elongation (Gates et al., 2017). GCN5 also directly acetylates some non-histone substrates, such as CDC6, cyclin A, PLK4 kinase, PGC1 (α and β), and regulates their respective cellular functions (Fournier et al., 2016; Kelly et al., 2009; Lerin et al., 2006; Orpinell et al., 2010; Paolinelli et al., 2009).

The identification of a GCN5-like histone acetyltransferase in the protozoan parasite *Tetrahymena thermophila* was a pioneering moment, showing that there is transcription modulation by histone-modifying proteins in parasites, with this protein subsequently being found to be important in other protozoan parasites, like *T. gondii* and *P. falciparum* (Brownell and Allis, 1995; Brownell et al., 1996; Croken et al., 2012; Merrick et al., 2012). Subsequently, these chromatin-modifying enzymes and their substrates have been demonstrated to play substantial roles in parasites, and there is some compelling evidence regarding the significance of epigenetic modification, including in cell cycle control, pathogenesis and virulence of pathogenic protozoans (Croken et al., 2012; Kirchner et al., 2016; Merrick et al., 2012). *P. falciparum* is one such protozoan parasite where these epigenetic mechanisms play a central role in the regulation

¹Special Centre for Molecular Medicine, Jawaharlal Nehru University, New Delhi 110067, India. ²School of Computational and Integrative Sciences, Jawaharlal Nehru University, New Delhi 110067, India. ³Centre for Cellular and Molecular Biology, Hyderabad, Telangana 500007, India. ⁴International Centre for Genetic Engineering and Biotechnology, New Delhi 110067, India.

*Author for correspondence (skdhar@mail.jnu.ac.in)

 K.B., 0000-0001-6213-8230; S.K.D., 0000-0002-9732-9456

of the timely controlled gene expression. The parasite completes its life cycle in two different hosts and requires a transition through different developmental stages. *P. falciparum* mastered this highly coordinated process by regulating the expression of the subset of genes required for the particular time point of their life cycle (Foth et al., 2011; Joice et al., 2013; Le Roch et al., 2004; Painter et al., 2017). HATs, histone deacetylases (HDACs) and histone methyltransferases (HMTs) are characterized as the major epigenetic regulators in the protozoan parasites (Croken et al., 2012). Inhibition of some of these enzyme functions through mutations, knockout analysis or small molecule inhibitors results in significant reduction in histone modifications, which confers a consequential effect on the transcription and translation process of the parasite (Agbor-Enoh et al., 2009; Chua et al., 2017; Kumar et al., 2017; Malmquist et al., 2012; Srivastava et al., 2014; Zhang et al., 2018).

P. falciparum GCN5 (PfGCN5) histone acetyltransferase is a ~170 kDa protein with a conserved acetylation domain and a bromodomain at the C-terminal region. Similar to the yeast homolog, it acetylates histone 3 at lysine residues 9 and 14 in the parasite (Fan et al., 2004b). Although the N-terminus of GCN5 shows less similarity among species, PfGCN5 contains an unusually long N-terminal region. The apicomplexan parasite *Toxoplasma* also contains such a long N-terminal sequence and its role in protein import to the nucleus has been characterized previously (Bhatti and Sullivan, 2005). However, the role of the N-terminus of PfGCN5 still remains elusive.

The only known role of PfGCN5 in the parasite is its acetylation activity towards histone H3 and how this acetylation mark influences gene expression. The functional importance of the H3K9Ac modification has been studied in *Plasmodium* through chromatin immunoprecipitation (ChIP)-sequencing (ChIP-seq) analysis, which has revealed its involvement in the activation of gene expression, including the invasion and virulence genes, whereas H3K14Ac function is not well understood in the parasite (Karmodiya et al., 2015; Salcedo-Amaya et al., 2009). ChIP-chip analysis of PfGCN5 suggests that it regulates only ~5% of gene expression in trophozoite-stage parasites (Cui et al., 2007). Unlike yeast, where GCN5 activity is considered to be dispensable for growth, *Plasmodium* GCN5 activity is essential for the parasite (Bushell et al., 2017; Zhang et al., 2018). In yeast, GCN5 forms two multi-subunit complexes known as the SAGA and ADA complexes (Grant et al., 1997). It has been suggested that these complexes are required for distinct nuclear HAT activity. Interestingly, PfADA2 has been characterized in *Plasmodium* and shown to interact with PfGCN5 *in vivo* (Fan et al., 2004a). This suggests that PfGCN5 also functions in a multi-subunit complex in the parasite. However, other homologs of SAGA complex components are not yet annotated in *Plasmodium*. Interestingly, *Toxoplasma gondii* expresses two GCN5 proteins (GCN5a and GCN5b), which are required for distinct functions in the parasite (Bhatti et al., 2006).

Regulation of GCN5 protein through posttranslational modification has been reported in other organisms. In diabetic db/db mouse hepatic cells, acetylation of GCN5 protein at lysine 549 (K549) causes impaired acetylation activity. Overexpression of the protein deacetylase Sirt6 in these cells leads to deacetylation of GCN5 and phosphorylation of S307 and T735 residues. Together, these modifications increase GCN5 activity on PGC-1 α protein, which further suppresses hepatic gluconeogenesis (Dominy et al., 2012).

Although PfGCN5 is considered to be essential in *P. falciparum*, functional regulation of this protein and its target genes are largely unknown. In the present study, we demonstrate a novel posttranslational modification of PfGCN5 that involves proteolytic

processing of full-length PfGCN5 before its transport to the nucleus. Most notably, we find that this processing occurs outside the nucleus at an unconventional site that has not been reported in the parasite or other eukaryotes. Using several molecular and cell biology techniques, we find the involvement of a cysteine class of protease present in the vicinity of parasite food vacuole preceded by possible engagement of the ER–Golgi secretory pathway. Furthermore, we performed ChIP-seq, which allowed us to identify the genome-wide occupancy of PfGCN5 for the first time. Intriguingly, the inhibition of PfGCN5 processing blocked the occupancy of the protein at the genome sites identified, highlighting the importance of proteolytic processing of the protein for its regulation and function. Overall, our study uncovers the existence of a novel regulatory mechanism for the modulation of nuclear gene expression in *P. falciparum*, which could be exploited as potential antimalarial target.

RESULTS

Expression of PfGCN5 histone acetyltransferase during asexual intraerythrocytic stages

The *P. falciparum* gene *gcn5* (*PfGCN5*) codes for a ~170 kDa acetyltransferase. The conserved acetyltransferase and bromodomain are present at the C-terminal region, whereas its N-terminal region is extensive and lacks any known conserved domain [Fig. 1A(I)]. In order to investigate the *in vivo* characteristics of PfGCN5, we generated antibodies against the C-terminal domain (1090–1465 amino acids) of the protein [Fig. 1A(II); Fig. S1A] and checked its specificity. First, we validated the specificity of these antibodies using lysate from bacteria expressing a recombinant PfGCN5 C-terminal domain. The immune sera, but not the pre-immune sera, successfully recognized a ~47 kDa band (expected size of recombinant protein) in the IPTG-induced sample and the purified protein sample (Fig. S1B). Furthermore, the specificity of antibodies was checked using protein lysate from asynchronous parasites. We detected a band at ~170 kDa, which is similar to the predicted size of full-length PfGCN5 protein. Additionally, we detected several other bands at ~40 kDa, 80 kDa, 90 kDa and 120 kDa (Fig. 1B, middle panel). Interestingly, it was observed, through repeated western blotting, that the bands at ~40 kDa, ~80 kDa and ~90 kDa were more prominent compared to the full-length band. The ~170 kDa band was not visible consistently in all the experiments, suggesting poor abundance of the full-length protein. Pre-immune sera did not detect any of these bands either in the parasite lysate or in red blood cell (RBC) lysate (Fig. 1B, left panel).

To further check the specificity of the antibodies, we carried out immunoprecipitation studies using the asynchronous parasite lysate with antibodies against PfGCN5 and found that all the protein bands present in the input lane were immunoprecipitated with antibodies against PfGCN5 but not with the pre-immune sera (Fig. 1C). We validated the immunoprecipitated sample through in-solution mass spectrometry (MS) analysis and found peptides from the C-terminal region of PfGCN5 (Fig. S1C). An earlier report on PfGCN5 suggests that PfADA2 interacts with PfGCN5 and this complex is required for the PfGCN5 acetylation function (Fan et al., 2004a). We also detected PfADA2 peptides in our MS analysis from the immunoprecipitated sample, further suggesting the specificity of our antibodies (Fig. S1C).

In order to confirm that the multiple bands observed in western blots are indeed part of PfGCN5 protein, we performed immunoprecipitation (IP) of PfGCN5 followed by western blotting and silver stain analysis. After confirming the positive IP in an immune sample by western blotting, we excised the corresponding bands from a silver-stained gel and subjected them

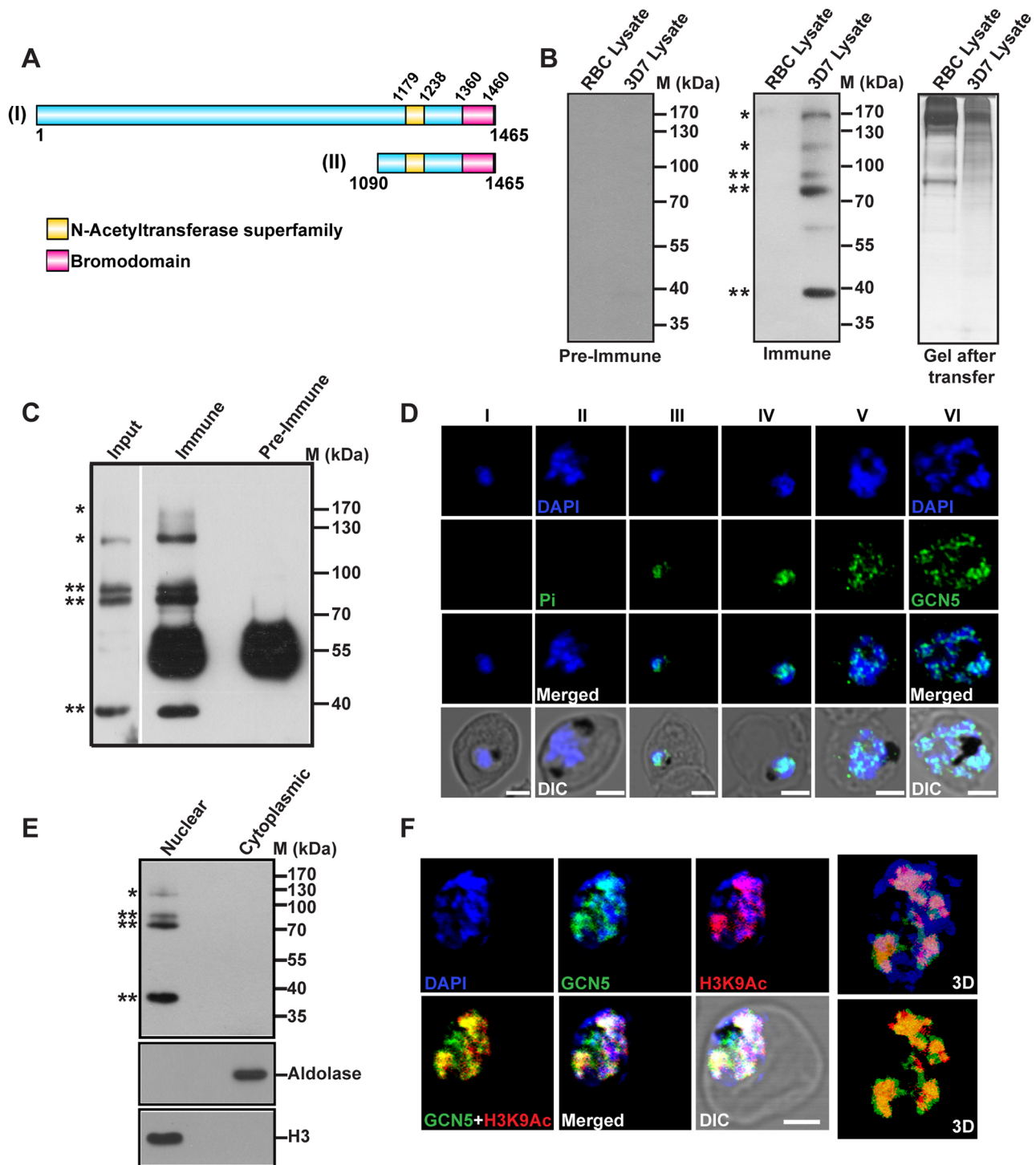


Fig. 1. Expression analysis of PfGCN5 in asexual blood stages. (A) Schematic representation of the full-length PfGCN5 protein with the conserved acetyltransferase (yellow) and bromodomain (pink) at C-terminal region (I). The region from amino acids 1090–1465 was used for the generation of the polyclonal antibodies against PfGCN5 (II). (B) Specificity of antibodies against PfGCN5 in mixed stage parasite lysate as analyzed through western blot analysis. Uninfected RBC lysate was taken as negative control. No cross-reactive band was observed in the pre-immune sera-treated blot. Multiple bands (* and **) were detected in the immune sera-treated blot, including the full-length band at ~170 kDa. The Coomassie-stained gel after transfer was used as loading control. The bands corresponding to ** were more prominent than those marked with * in repeated western blots experiments. (C) Immunoprecipitation of endogenous PfGCN5 protein using antibodies against PfGCN5 from parasite lysate. Western blot analysis showed the presence of multiple bands in the lane corresponding to immune sera, similar to the input lane, but not in pre-immune sera. (D) Immunofluorescence analysis of PfGCN5 in different parasite stages using pre-immune sera (I, II, Pi) and immune PfGCN5 sera (III–VI). Alexa Fluor 488-tagged secondary antibodies were used for the detection of PfGCN5. DAPI was used to stain the nucleus. (E) Subcellular fractionation followed by western blot analysis shows the nuclear enrichment of PfGCN5 bands. PfH3 and PfAldolase were used as nuclear and cytoplasmic controls, respectively. (F) Colocalization of PfGCN5 and PfH3K9Ac in fixed parasites using antibodies against respective proteins. The nuclei were stained with DAPI. Alexa Fluor 488 and Alexa Fluor 594-tagged secondary antibodies were used to detect PfGCN5 (green) and PfH3K9Ac (red) respectively. 3D views of selected images are shown on extreme right for better clarity. See Movie 1 for movies of these 3D reconstructed images. The position of molecular mass markers [M (kDa)] are indicated on the right side of each western blot. Scale bars: 2 μ m.

to mass spectrometric analysis. We found multiple PfGCN5 peptides from each region (Fig. S1D, region I, II and IV) confirming that the bands observed in the western blot are indeed generated from full-length PfGCN5 protein (Fig. S1D). A control region from the immune lane was also taken for MS analysis. However, we could not detect any PfGCN5 peptide from this region (Fig. S1D, region III, yellow circle). These results confirm that the multiple bands present in the western blot indeed correspond to PfGCN5.

In order to check the stage-specific expression and intracellular localization of PfGCN5, immunofluorescence analysis was carried out in different parasite stages. Pre-immune sera did not give any signal in the parasite [Fig. 1D(I,II)]. Fig. 1D shows the expression of PfGCN5 in all the stages. During the early stages of development, the PfGCN5 signal was distributed over the nuclear DAPI signal [Fig. 1D(III,IV)] but it showed a more punctate pattern over the nucleus during later stages of development [Fig. 1D(V,VI)]. Furthermore, a subcellular fractionation experiment from mixed stage parasites showed the presence of all the fragments of PfGCN5 in the nuclear fraction (Fig. 1E), corroborating the immunofluorescence assay results. Antibodies against histone H3 and PfAldolase were used as controls for the authenticity of the nuclear and cytoplasmic fractions.

Additionally, we performed colocalization studies using monoclonal antibodies against H3K9Ac and polyclonal antibodies against PfGCN5. The results indicated a significant colocalization between these two proteins (Pearson's correlation coefficient of 0.79). Some independent PfGCN5 signals were also observed, which may reflect that PfGCN5 has separate functions apart from histone acetylation (Fig. 1F). Together, these results suggest that antibodies raised against PfGCN5 are specific for PfGCN5 protein, which is expressed throughout the asexual blood stage. Our results also suggest that there could be processing of the full-length protein because multiple bands were found in the western blot.

PfGCN5 is proteolytically processed by a cysteine protease-like enzyme

The coding region of *PfGCN5* has three introns in the region encoding its C-terminal. However, northern blot analysis of the total RNA from asynchronous asexual stage showed a single mRNA product at ~5.4 kb, suggesting the absence of splice variant(s) in the asexual cycle (Fan et al., 2004b). Thus, the appearance of multiple shorter fragments in the western blot was intriguing. We hypothesized that these fragments are generated through proteolytic processing of the full-length PfGCN5 protein. In order to look for possible proteases responsible for this processing event, we used the protease specificity prediction server PROSPER (<https://prosper.erc.monash.edu.au/home.html>), which predicted the involvement of cysteine protease family in the cleavage of PfGCN5 (data not shown). For experimental validation, we treated early trophozoite stage parasites with a specific cysteine protease inhibitor E64d (8 μ M) or DMSO control for 10 h. E64d treatment showed a dramatic increase in the intensity of the full-length band (~170 kDa) with the disappearance of the lower molecular mass fragments (Fig. 2A). However, the presence of these shorter fragments was unchanged in the DMSO-treated parasite samples. To further confirm that this processing event was indeed cysteine protease specific, we also treated the parasites with the aspartyl-protease inhibitor Pepstatin A (75 μ M for 10 h). Interestingly, Pepstatin A was unable to block the processing of full-length protein, as occurred for E64d (Fig. 2A). Therefore, these results indicate the involvement of a cysteine protease-like enzyme in the processing of PfGCN5.

A recent study has shown that MG132 can also block the cysteine protease activity in parasites as does cysteine protease inhibitor E64d (Prasad et al., 2013). To further confirm the cysteine protease-mediated processing of PfGCN5, we treated the parasites with various concentrations of MG132 for 6 h. MG132 successfully stabilized the full-length protein and reduced the intensity of shorter fragments in the western blot, as was observed with E64d treatment

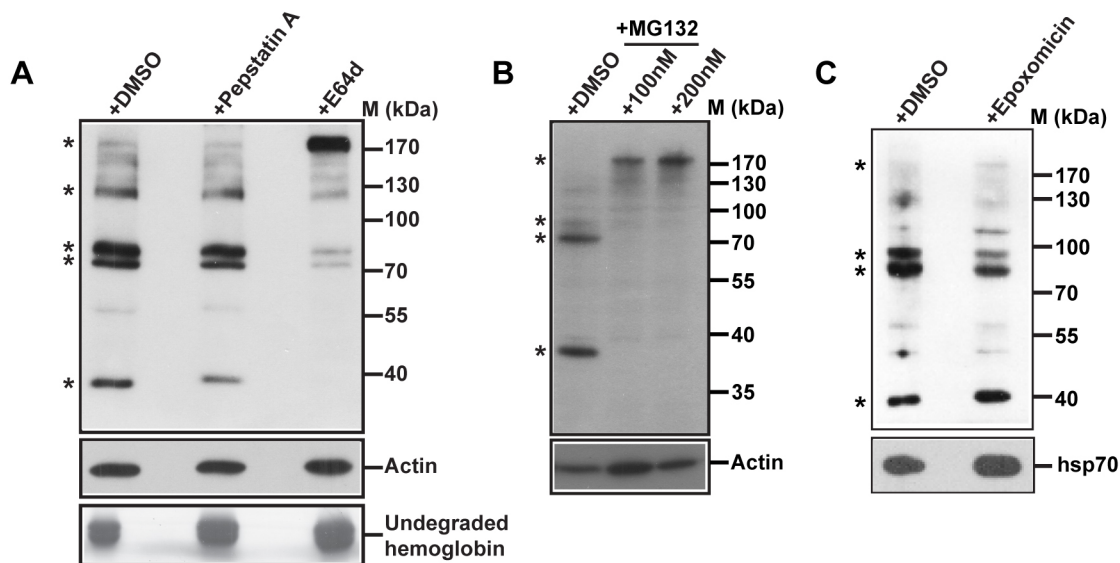


Fig. 2. Cysteine protease-mediated processing of PfGCN5. (A) Western blot analysis was carried out using lysate prepared from E64d, pepstatin A or DMSO-treated parasites. Antibodies against PfGCN5 were used for the detection of full-length or processed forms of PfGCN5 protein. Actin was used as loading control (middle panel). The bottom panel shows a Coomassie-stained gel with amount of accumulated hemoglobin in each sample. (B) Effect of MG132 on PfGCN5 processing. Trophozoite stage parasites treated with DMSO or MG132 (100 nM or 200 nM) were used for western blot analysis. The results show the appearance of full-length PfGCN5 in the presence of MG132 but not with DMSO treatment. Actin was used as a loading control. (C) Processing of PfGCN5 is not affected by the proteasomal inhibitor epoxomicin. No stabilization of full-length protein was observed in epoxomicin (20 nM)-treated parasites. Hsp70 was used as loading control in this experiment. Asterisks indicate the multiple bands of PfGCN5.

(Fig. 2B). To exclude the possibility that this was caused by inhibition of proteasomal activity, given that MG132 is known to be a prominent proteasome inhibitor (Lee and Goldberg, 1998), we also performed experiments with the proteasome-specific inhibitor epoxomicin (Meng et al., 1999). Epoxomicin was unable to block the processing of the protein, while accumulation of ubiquitylated proteins was observed under the same experimental conditions (Fig. 2C and see also Fig. S2). Altogether, our results provide strong evidence that the processing of full-length PfGCN5 protein is mediated by a cysteine protease-like enzyme.

The processing of PfGCN5 occurs at the vicinity of digestive vacuole of the parasite

In order to investigate the possible *in vivo* location of processing of PfGCN5, we performed an immunofluorescence assay using antibodies against PfGCN5 following treatment of the parasites with cysteine protease inhibitors (MG132 and E64d). To our surprise, in treated parasites the PfGCN5 signal was detected mostly around the hemozoin-containing area, which was totally different from the punctate nuclear localization of the same protein in DMSO-treated control parasites (Fig. 3A). Hemozoin deposition takes place in the parasite food vacuole, the equivalent of the lysosome in *Plasmodium*, wherein hemoglobin is degraded by multiple proteases, including cysteine and aspartic proteases. Hence, we further evaluated the possible association of an unprocessed form of PfGCN5 with the food vacuole. Previously, it has been reported that the autophagy protein Atg18 is localized in close vicinity to the food vacuole (Bansal et al., 2017). Immunocolocalization of PfGCN5 in a parasite line expressing GFP–PfAtg18 (Fig. S5) showed significant colocalization between PfGCN5 and Atg18 (Pearson's correlation coefficient of 0.67) around the food vacuole in the presence of MG132 (Fig. 3B, second panel from the top). No such colocalization between GCN5 and Atg18 was observed in control DMSO-treated parasites (Fig. 3B, top panel). As a control, we also checked the localization of PfActin, which did not change at all in the presence or absence of MG132 (Fig. 3B, bottom two panels), suggesting that the peripheral food vacuolar localization of PfGCN5 is not a random event for any protein but specific for PfGCN5.

Localization of PfGCN5 as a ring-like structure surrounding the food vacuole in the treated sample prompted us to investigate its association with the membrane of the food vacuole. For this purpose, an MG132-treated parasite pellet was subjected to the subcellular fractionation using the protocol described in the Materials and Methods. The full-length PfGCN5 protein was detected mainly in the Na_2CO_3 extractable fraction, which suggests its presence as a peripheral membrane-bound protein surrounding the food vacuole (Fig. S3). As a control, we used antibodies against PfAldolase, which was only present in the soluble fraction confirming the authenticity of the extraction process. Coomassie staining was used to show the presence of a similar amount of proteins in all lanes.

Furthermore, direct evidence for the food vacuolar localization of unprocessed PfGCN5 was obtained by immuno-electron microscopy (immuno-EM) with antibodies against PfGCN5. The results indicated the predominant presence of PfGCN5 (as reflected by gold particle deposition) in the nucleus and not the food vacuolar region in control DMSO-treated parasites (Fig. 3C, left panels). In sharp contrast to what was seen in DMSO-treated parasites, the distribution of gold particles in MG132-treated parasites was changed. In these parasites, the majority of the gold particles were in the food vacuolar region with only a minority being present in the nuclear region (Fig. 3C, right panels). A schematic diagram that reflects the abundance of the gold

particles in the subcellular milieu shows how the majority of the PfGCN5 signal could originate from the periphery of the food vacuole in the treated parasites (Fig. 3D). These results indeed suggest that the full-length protein gets processed at the vicinity of the food vacuole, possibly by a food vacuolar cysteine protease.

To check the association of full-length PfGCN5 protein with the parasite food vacuole, we isolated the food vacuole from MG132-treated parasites following the standard protocol as described in the Materials and Methods. The full-length protein was detected in the whole-cell parasite lysate and food-vacuole enriched fraction, suggesting the association of unprocessed protein with the parasite food vacuole (Fig. 3E, upper left). GFP–PfAtg18 was also present in the food vacuole-enriched fraction and served as positive control (Fig. 3E, right blot). However, the cytoplasmic protein PfAldoase was only present in the whole parasite lysate but not in the food vacuole-enriched lysate, indicating the purity of food vacuole enriched fraction (Fig. 3E, bottom left).

The full-length PfGCN5 traffics to the food vacuole via the ER–Golgi secretory pathway

The above results indicate that the full-length PfGCN5 is associated with the food vacuole where it gets processed by a cysteine protease before it is targeted to the nucleus. Previous reports on food vacuole proteins like PfPM II and PfCRT have shown that they must enter the secretory pathway before reaching the food vacuole (Klemba et al., 2004; Kuhn et al., 2010). Therefore, we wondered whether, following the synthesis of the full-length PfGCN5 protein, it traffics via ER–Golgi-mediated secretory pathway to the food vacuole. The well-known inhibitor of ER–Golgi transport pathway, brefeldin A (BFA), has been used in *P. falciparum* extensively (Benting et al., 1994; Klemba et al., 2004; Kuhn et al., 2010; Sharma et al., 2018). We treated synchronized trophozoite-stage parasites with BFA (5 $\mu\text{g}/\text{ml}$) and ethanol for 12 h. Interestingly, BFA-treated parasites showed the stabilization of the full-length PfGCN5 protein, similar to MG132 treatment (Fig. 4A, top panel). It should be noted that the effect of BFA was also observed after a shorter incubation time period (6 h; data not shown) but a more profound effect was observed following a 12 h treatment. In contrast, the parasites treated with ethanol (control) did not show any effect on PfGCN5 processing (Fig. 4A, top panel). It has been shown that the transport of nuclear-encoded apicoplast-targeted proteins are sensitive to BFA (Tonkin et al., 2006). We observed similar effect of BFA on PfSSB, where unprocessed PfSSB protein (containing the transit peptide) was stabilized by BFA but not by ethanol or MG132 (Fig. 4A, second panel from bottom). The effect of BFA on SSB processing indeed confirmed its interference with the ER–Golgi network of the parasites. However, the ER resident protein Bip was not affected by BFA treatment, suggesting that the unprocessed full-length PfGCN5 protein travels through ER to food vacuole for processing (Fig. 4A, second panel from top).

Furthermore, we performed immunofluorescence analysis in BFA-treated parasites using antibodies against PfGCN5 and the ER-resident protein Bip. In control ethanol-treated parasites, the PfGCN5 signal was mostly colocalized with the nuclear DAPI signal, and was quite distinct from the Bip signal present at the nuclear periphery of (Fig. 4B). However, BFA-treated parasites showed significant colocalization of PfGCN5 and Bip (Pearson's correlation coefficient of 0.74), suggesting a block in trafficking of PfGCN5 (Fig. 4B, lower row and enlargements).

The above results indeed highlight the importance of the ER–Golgi network for trafficking of PfGCN5 to the nucleus via the parasite food vacuole.

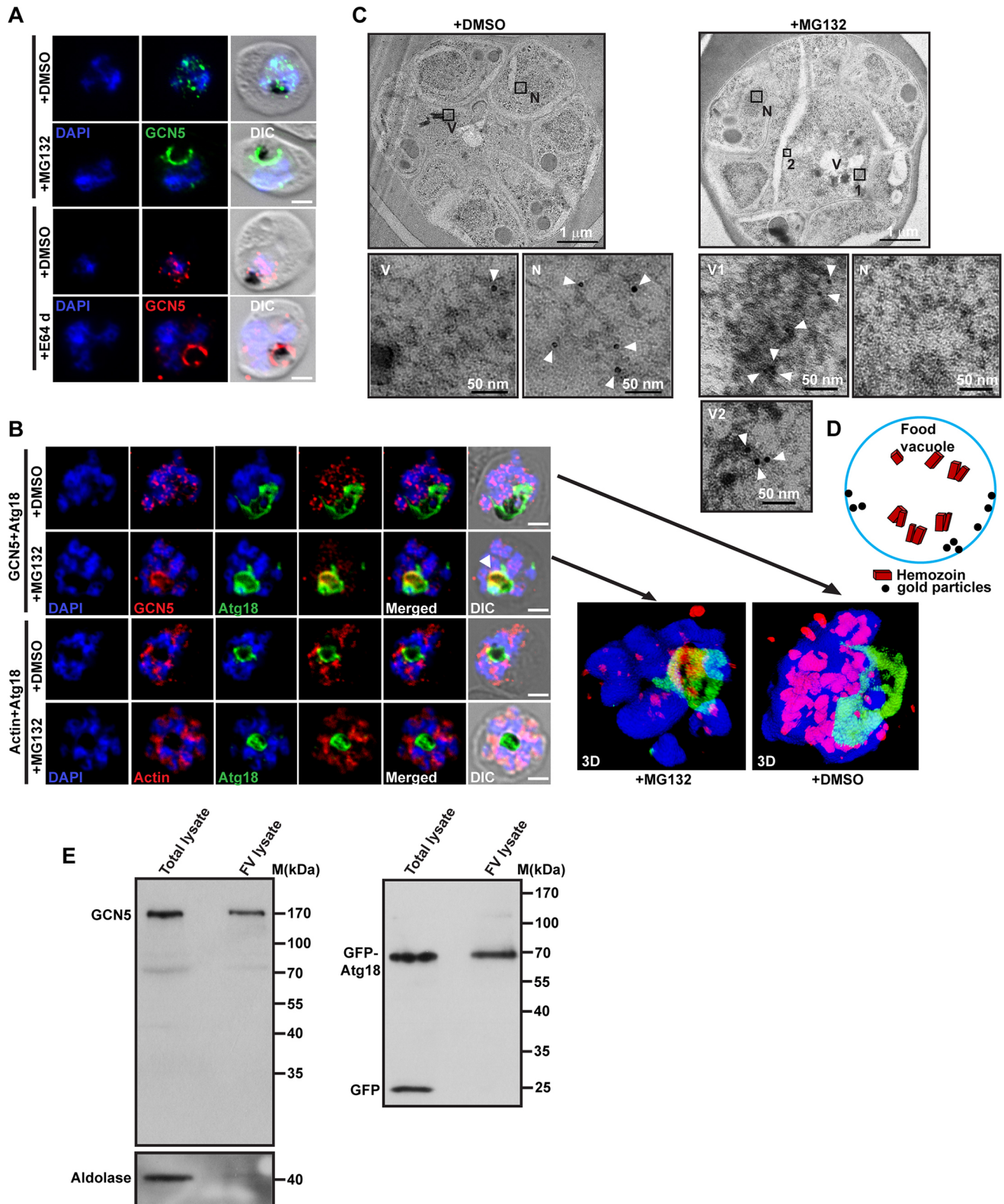


Fig. 3. See next page for legend.

ChIP-seq analysis of PfGCN5 reveals the genome-wide occupancy of the protein

In *P. falciparum*, GCN5 acetylates histone 3 (H3) at lysine 9 and 14 residues and regulates the gene expression of the parasite. However, genome-wide binding of PfGCN5 had not been previously studied.

Moreover, we wanted to check the functional significance of PfGCN5 processing to where it bound to the genome regions and its histone acetylation activity at those regions. To gain further insight into this, we performed a genome-wide ChIP-seq analysis on trophozoite- and schizont-stage-enriched parasites using antibodies

Fig. 3. Immunolocalization of PfGCN5 following inhibition of processing of the protein. (A) Immunofluorescence analysis of PfGCN5 in parasites treated with DMSO (control), MG132 (100 nM) and E64d (10 μ M). Following inhibitor treatment, fixed parasites were subjected to an immunofluorescence assay using antibodies against PfGCN5 followed by secondary antibodies tagged with Alexa Fluor 488 or Alexa Fluor 568 for MG132-treated or E64d-treated parasites, respectively. DAPI was used to stain the nuclei of the parasite. Scale bars: 2 μ m. (B) Double immunofluorescence analysis was carried out using GFP–PfAtg18-expressing MG132 (100 nM)-treated parasites in the presence of antibodies against PfGCN5, GFP and PfActin (in combination) followed by respective secondary antibodies tagged with Alexa Fluor 594 (PfGCN5 and PfActin) or Alexa Fluor 488 (GFP–Atg18). DAPI was used to stain nuclei. Colocalization of PfGCN5 with PfAtg18 is indicated by the white arrowhead; no colocalization was seen with control actin. The right panels show the 3D reconstruction of the selected images from the left panel. See Movies 2 and 3 for movies for these 3D reconstructed images. Scale bars: 2 μ m. (C) Immuno-EM images to detect the *in vivo* localization of PfGCN5 protein in untreated and MG132-treated parasites. Secondary antibodies tagged with 10-nm-gold particle against primary antibodies (PfGCN5) were used for detection. Schizont stage parasites with a nucleus and a food vacuole, indicated as 'N' and 'V', respectively, in DMSO- and MG132-treated parasites are shown. The selected areas (squares) are also shown at the higher magnification at the bottom (N, V and N, V1, V2 for untreated and drug-treated parasites, respectively). Localization of protein is highlighted with white arrowheads. (D) Schematic diagram shows the localization of gold particles around the food vacuole of MG132 treated parasite as shown in C. (E) Western blot analysis of whole-parasite lysate (total lysate) and food vacuole-enriched fraction (FV lysate) using antibodies against PfGCN5 (upper left blot), GFP (right blot) and PfAldolase (bottom left blot) proteins. Bands corresponding to each protein are indicated on the left side of the blot.

against PfGCN5. The results obtained here were very astounding, as the binding sites were not restricted to specific regions, but rather enriched throughout the genome (Fig. 5A). The total number of reads generated from the anti-GCN5 immunoprecipitated sample was ~25 million. Approximately, 20 million reads were successfully aligned to the *P. falciparum* genome using Bowtie2 (version 2.1.0). Furthermore, we estimated the peak density (peak/Mb) and identified ~140 narrow peaks/Mb for total genome size. Here, narrow peak refers to a possible GCN5-binding site. A representative view of the chromosome-wide distribution of PfGCN5 (chip/input) is shown in Fig. 5A. Thorough analysis of the data revealed 3400 narrow peaks, and the majority of the binding sites were near the vicinity of promoter regions (~51%). The remaining sites had a more-or-less uniform distribution [i.e. exons (~19%), transcription termination sites (TTS) (~15%) and intergenic regions (~15%)] (Fig. 5B; Table S1).

Furthermore, we carried out a gene ontology (GO) study of PfGCN5-binding sites and found that genes that are in the vicinity of PfGCN5-binding sites are involved in diverse biological functions (Fig. 5C). Interestingly, the majority of the genes are related to gene transcription, host cell entry and host cell reprogramming functions. Altogether, these observations elucidate a general overview on PfGCN5-binding sites across the genome and some idea about the genes that are possibly regulated by this protein. However, a detailed analysis needs to be done, which is not the primary focus of our present study.

Genome-wide occupancy of the histone H3K9Ac mark has been studied in *P. falciparum* (Bártfai et al., 2010; Karmodiya et al., 2015). H3K9Ac together with H3K4me3 is mainly enriched in promoter regions in the parasites (Bártfai et al., 2010). To confirm if H3K9Ac and GCN5 are present in the same genomic regions, we co-aligned the PfGCN5 ChIP-seq data with publicly available H3K9Ac ChIP-seq data. A representative view of this co-alignment is shown in Fig. S4. Interestingly, the result showed ~70% of PfGCN5 peaks fall within 1 kb upstream or downstream

of H3K9Ac sites. These results indeed suggest that majority of the PfGCN5-binding sites are correlated with its histone H3 acetylation function. In contrast, 30% of PfGCN5-occupied sites are unique to PfGCN5, suggesting some separate function of this protein.

To validate our ChIP-seq result, we randomly selected few GCN5 binding sites (see Table S2 for coordinates) and performed ChIP-quantitative PCR in asynchronous stage parasites using antibodies against PfGCN5. As seen in Fig. 5D, enrichment of PfGCN5 at these sites is evident compared to the binding at control region. Notably, the binding efficiency of PfGCN5 at these sites is highly correlated with the data we obtained from the ChIP-seq experiment.

Processing of PfGCN5 is necessary for its nuclear acetylation function

As mentioned earlier, PfGCN5 is responsible for the acetylation of histone H3 at lysine residues 9 and 14 (H3K9Ac and H3K14Ac) (Fan et al., 2004b). Moreover, acetylation of H3 at these sites, especially H3K9Ac, is necessary for the expression of active genes in the asexual stages of the parasite (Salcedo-Amaya et al., 2009). Additionally, several PfGCN5-specific inhibitors were employed in the *in vitro* parasite culture which showed inhibition of the GCN5 acetylation activity leading to downregulation of H3K9 acetylation and reduced gene expression (Srivastava et al., 2014). To examine the importance of the PfGCN5 processing for its enzymatic activity, we treated the parasites with MG132 and checked the acetylation status of H3K9. Intriguingly, the acetylation level of H3K9 went down significantly in the presence of increasing amount of MG132 (~50% in 60 nM) compared to DMSO-treated parasites (Fig. 6A, top panel, and B). A previously characterized PfGCN5 inhibitor, embelin, also downregulated H3K9 acetylation under the same experimental conditions, serving as a positive control (Fig. 6A, top panel) (Srivastava et al., 2014). Furthermore, we also evaluated the status of PfGCN5 processing in these samples. MG132 indeed blocked the PfGCN5 processing with the appearance of the strong full-length protein band. Neither DMSO nor embelin could inhibit the PfGCN5 processing event (Fig. 6A, bottom panel). PfH3 was used as the loading control for the western blot analysis. It is intriguing that different inhibitors working in different pathways lead to the inhibition of the PfGCN5 activity. While embelin works directly on the PfGCN5 enzymatic activity, MG132 affects PfGCN5 activity by interfering with its proteolytic processing.

Subsequently, we evaluated the loading of the processed (untreated) and unprocessed (MG132 treated) form of PfGCN5 at the selected promoter regions that we identified from the ChIP-seq results. Synchronized early trophozoite stage (20 \pm 5) parasites were treated with 60 nM MG132 or DMSO for 12 h and then subjected to a chromatin immunoprecipitation assay using antibodies against PfGCN5, H3K9Ac and histone H3 in separate reactions. For validation, we selected four high to moderate PfGCN5-binding gene promoter regions. In DMSO-treated control parasites, we observed varied binding of PfGCN5 at these regions while MG132 treatment drastically reduced the PfGCN5 occupancy at the same sites (Fig. 6C,D). Similarly, the H3K9Ac level showed significant reduction following MG132 treatment at the same promoters, as compared to the level in DMSO-treated parasites. These results suggest that the inhibition of PfGCN5 processing drastically compromises its occupancy at the promoter regions with concomitant downregulation of H3K9Ac level at the same sites, possibly due to the unavailability of the active processed form in the nucleus following drug treatment.

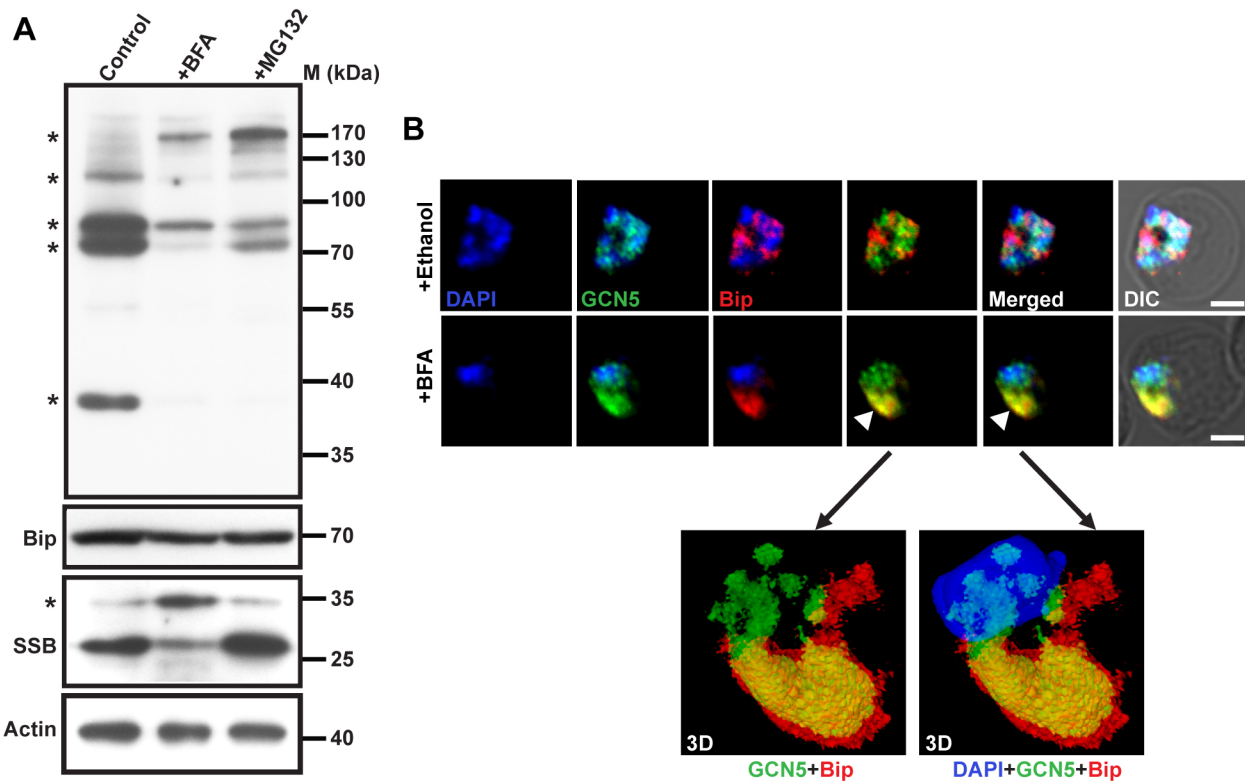


Fig. 4. PfGCN5 protein gets stabilized and redistributed to the ER compartment upon treatment with brefeldin A. (A) Effect of BFA (5 μ g/ml for 12 h) on PfGCN5 showing the stabilization of full-length PfGCN5 protein, similar to what is seen for MG132-treated (60 nM for 12 h) parasites (top panel). The effect of BFA on Bip and SSB are shown as a positive control for this experiment (middle panels). Actin was used to show the equal loading of proteins in each lane (bottom panel). Asterisks indicate the multiple bands of PfGCN5 (top) and SSB. (B) Effect of BFA on the localization of PfGCN5 protein in fixed parasites. The ER-resident protein Bip was used as an ER marker. Immunofluorescence analysis shows different distribution of PfGCN5 and Bip in ethanol-treated cells (top panel). BFA-treated parasites show significant colocalization of the above two proteins (indicated by the white arrowhead; middle panels). The enlarged images show 3D reconstructions of the selected images from the middle panels. See Movie 4 for movies of these 3D reconstructed images. Scale bars: 2 μ m.

DISCUSSION

In the present study, we report the existence of a novel pathway in nuclear gene regulation of malaria parasites through proteolytic processing of nuclear PfGCN5 by a food vacuolar cysteine protease. We observed several processed forms of PfGCN5 (~40 kDa, 80 kDa, 90 kDa and 120 kDa) that were present throughout the asexual stage of the parasite while the full-length protein was barely detectable. Although *Pfgen5* contains three introns at the 3' end of the gene, no splicing event has been reported in asexual blood stage and only a single mRNA corresponding to the full-length transcript was detected in northern blot analysis (Fan et al., 2004b). However, alternative splicing events of GCN5 transcripts have been observed in mouse and human cells (Smith et al., 1998). These alternative spliced variants are translated into functionally distinct protein products that are part of various protein complexes. It is possible that *P. falciparum* has adopted processing of the PfGCN5 protein instead of alternative splicing of PfGCN5 transcripts, highlighting the complex regulation of the parasite proteins. It needs to be explored further whether the alternative splicing events occur in other stages of the parasite.

The conserved HAT domain and bromodomain of PfGCN5 are present at the C-terminal region of the protein. The antibodies against PfGCN5 were generated against the C-terminal domain of the protein, which detected all the multiple PfGCN5 forms, suggesting that these forms at least contain either the full C-terminal region or some part of the C-terminal region of the protein. A recent study has shown that the C-terminal domain of PfGCN5 (amino acids 1090–

1465) is sufficient for its *in vivo* acetylation activity in the nucleus (Xiao et al., 2019). These findings suggest possible functional role of the fragments detected by western blot in the nucleus. It has been reported that the apicomplexan parasite *T. gondii* expresses two GCN5 acetyltransferases (TgGCN5A and TgGCN5B) proteins (Bhatti et al., 2006). Among them only TgGCN5B is essential for the parasite. Moreover, the yeast GCN5 acetyltransferase is known to be part of at least two multi-subunit complexes that are functionally active (Grant et al., 1997). It is possible that the multiple forms of PfGCN5 are required to form functionally distinct complexes in the parasite, which requires further experimental validation that is beyond the scope of the present study.

We also demonstrate that the proteolytic cleavage of PfGCN5 is mediated by a cysteine class protease that is associated with the food vacuole. Processing of proteins is very important for the parasite and it has been mainly studied with respect to hemoglobin digestion and merozoite surface protein maturation. In a recent study, we have shown that the replication protein PforC2 goes through an ER-associated proteolytic processing pathway to attain its mature form (Sharma et al., 2018). Another study on histone H3 shows that PfH3 protein is 'clipped' by a nuclear protease in asexual blood stage and this cleaved H3 form is enriched at the upstream regions of few DNA replication/repair genes (Herrera-Solorio et al., 2019). However, cleaving of a nuclear protein by a food vacuole protease is unique to parasites and does not generally occur in eukaryotic organisms. Interestingly, malaria parasites express a large number of high molecular mass proteins. Only few

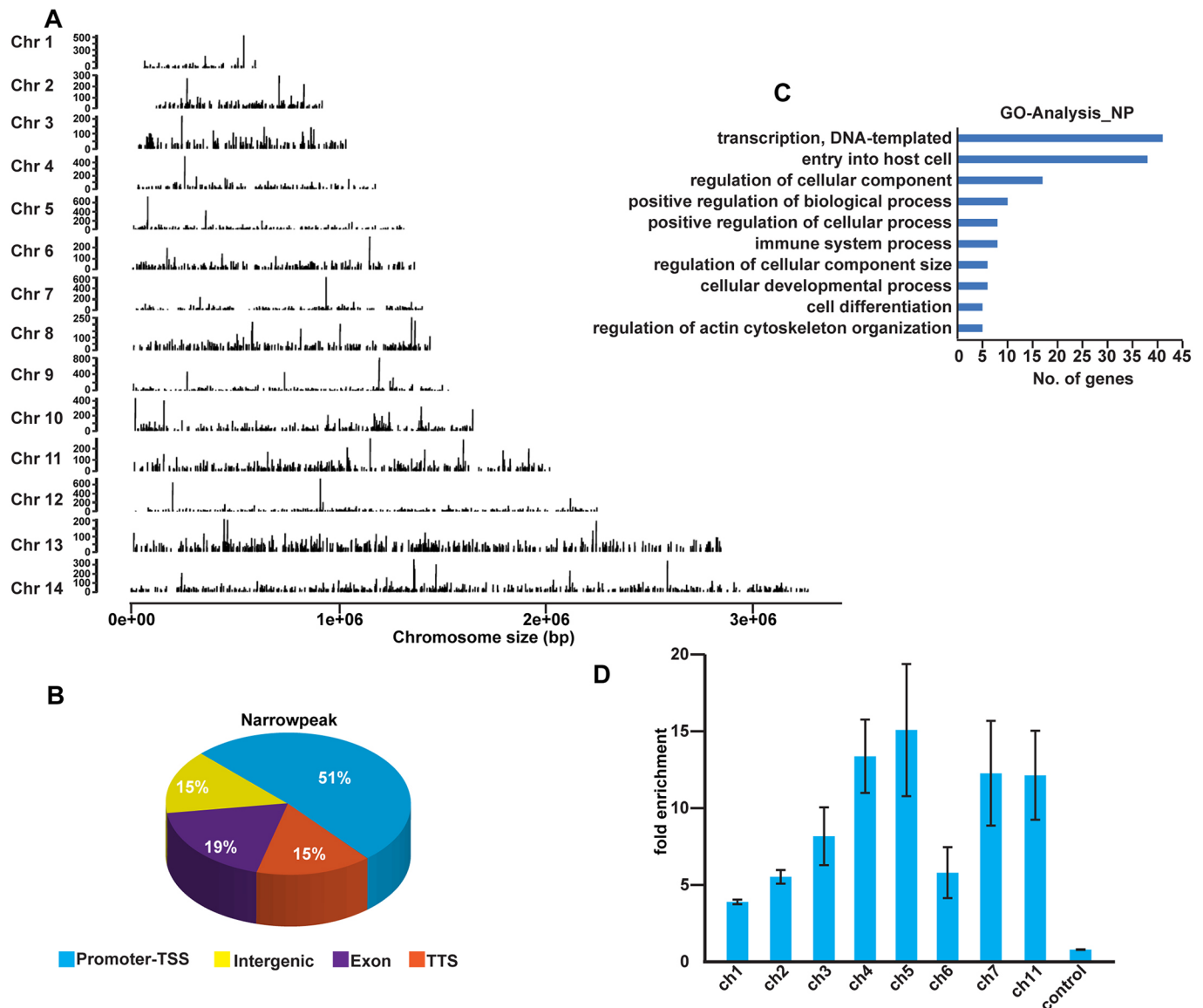


Fig. 5. Characterization of genome-wide binding sites of PfGCN5. (A) Genome-wide occupancy of GCN5 acetyltransferase in the 14 chromosomes of *P. falciparum*. Peaks displayed here are the relative enrichment of PfGCN5 (immunoprecipitated DNA) compared to the input (total DNA). The x-axis denotes the chromosome size (base pair) and the y-axis denotes the peak score. (B) Distribution of total peaks over all the chromosomal regions. (C) GO analysis (biological processes) of PfGCN5 occupied regions. The genes in the vicinity or nearby regions of the narrow peak were taken for GO enrichment and pathway analysis. The gene ontology and pathway analysis of these genes were obtained from PlasmoDB database using its annotation file. The highly enriched biological processes, molecular function and pathways are shown here, with the x-axis representing the number of genes corresponding to each pathway. (D) Validation of the selected PfGCN5-binding sites (see Table S2 for coordinates) through ChIP-qPCR analysis; the chromosome no. from which the regions were selected is indicated. The y-axis represents the enrichment of PfGCN5 over input at each region. Results are mean \pm s.e.m. from two independent experiments each repeated at least twice.

of those proteins are reported to undergo proteolytic processing to date. For example, the parasite MSP1 protein undergoes extensive proteolytic processing and these processed proteins have been reported to be part of several functionally different protein complexes (Blackman et al., 1991; Lin et al., 2016). However, constitutive processing of nuclear proteins like PfGCN5 and PfORC2 indicate that it is possible that other large nuclear proteins also undergo processing to achieve their mature functional form.

The *P. falciparum* genome encodes 27 putative cysteine proteases and their role in essential pathways like invasion, egress, and hemoglobin degradation have been investigated (Siqueira-Neto et al., 2018). The falcipain cysteine proteases (falcipain 1, 2a, 2b

and 3) and dipeptidylaminopeptidase 1 (DPAP1) have been shown to be localized to the food vacuole. Among them, falcipain 3 and DPAP1 are essential in the asexual cycle of the parasite. These proteases degrade hemoglobin in the food vacuole as their substrate. Falcipains have also been implicated in processing of plasmepsins and the erythrocyte cytoskeleton. Since DPAP1 is an amino peptidase that cleaves dipeptides from the N-terminus of oligopeptides (Klemba et al., 2004), it is unlikely to mediate processing of PfGCN5. However, falcipain 1, falcipain 2a and falcipain 2b have been shown to be nonessential (Sijwali et al., 2006), whereas PfGCN5 is essential. Therefore, it is unlikely that the above falcipains are the primary mediators for the processing of PfGCN5. Falcipain 3 appears to be essential but it remains

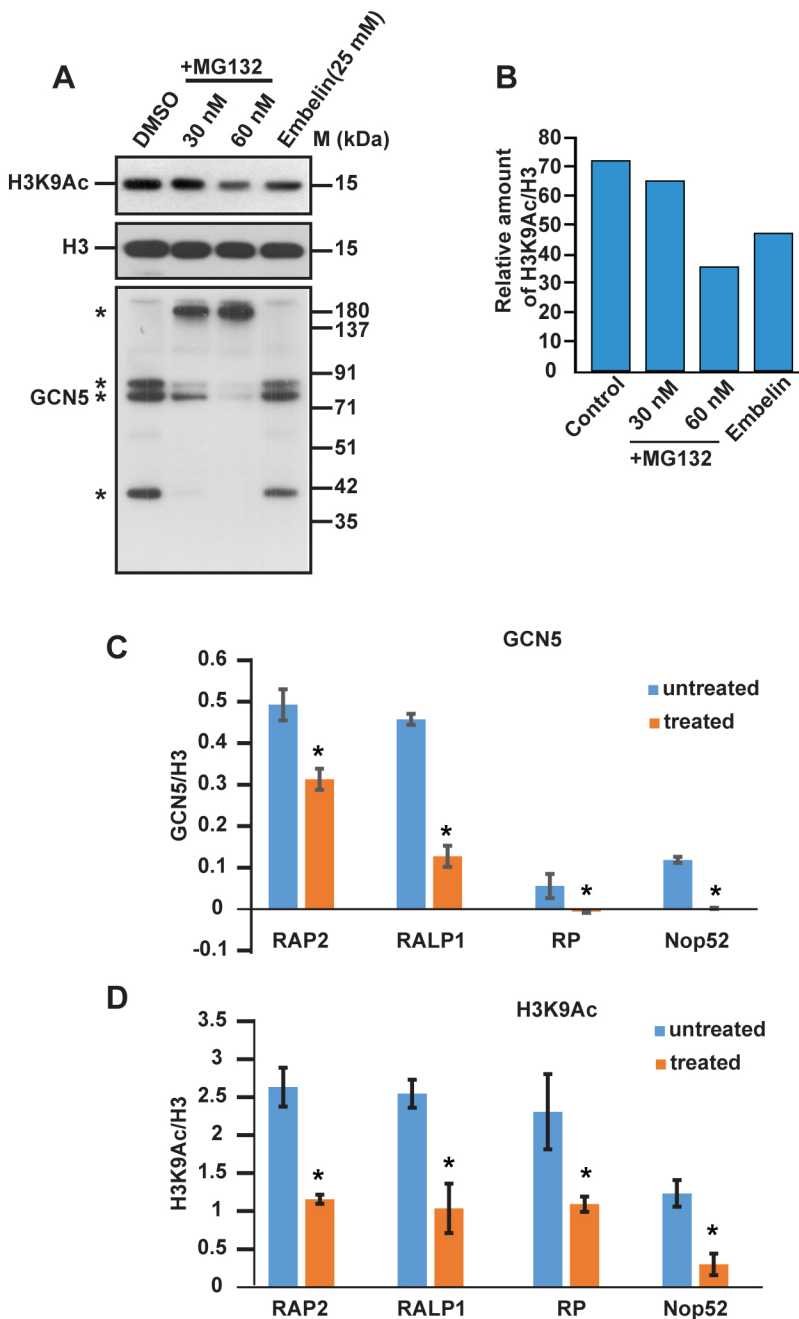


Fig. 6. Maturation of PfGCN5 is required for its activity.

(A) Western blot analysis showing the effect of MG132 (30 nM and 60 nM) and embelin (25 mM) on H3K9Ac level in the parasites compared to DMSO-treated parasites. Histone H3 was used as the loading control. The bottom panel shows the status of PfGCN5 protein in different samples as above. Asterisks indicates the multiple bands of PfGCN5 protein. (B) A densitometry analysis of the blot in A is plotted as a bar graph that shows the relative amount of H3K9Ac (to histone H3) protein present in all the samples. (C,D) ChIP-qPCR analysis was performed to check the relative occupancy of PfGCN5 and PfH3K9Ac at selected promoter regions from MG132-treated and untreated parasites using antibodies against PfGCN5 and H3K9Ac, respectively. The results indicate that the loading of PfGCN5 is affected in the presence of MG132 with a similar effect on the acetylation of PfH3 (H3K9Ac) at these promoter regions. All the above experiments were repeated at least twice. Results are mean \pm s.e.m. from two independent experiments each repeated at least twice. * $P < 0.05$ (Student's *t*-test).

elusive at this stage whether it is the PfGCN5-processing cysteine protease.

Another interesting observation here is that full-length PfGCN5 protein is sensitive to BFA treatment suggesting that following protein synthesis the full-length protein enters the ER-Golgi secretory pathway prior to processing in the vicinity of food vacuole. This result was anticipated due to the fact that other food vacuole proteins, like plasmepsins and falcipains, also follow a similar pathway before reaching the food vacuole (Klemba et al., 2004; Subramanian et al., 2007). However, we are intrigued to see the emerging role of *Plasmodium* ER in nuclear gene regulation. In other organisms, many membrane-bound transcription factors have been reported to enter nucleus via an ER-Golgi-related trafficking pathway. However, processing of these transcription factors is dependent on certain physiological cues, like ER stress or ligand-mediated activation. For example, proteins like epidermal growth

factor receptor (EGFR), suppressor of Ty 23 (SPT23), myelin regulatory factor (MYRF), MrfA, SREBP, basic leucine zipper (bZIP), ATF6 and OASIS all follow an ER-Golgi trafficking pathway before reaching the nucleus (Liu et al., 2018).

ChIP-seq results shed some light into the genome-wide occupancy of GCN5 acetyltransferase in the asexual stage of the parasite. Our data corroborated earlier ChIP-seq results on H3K9Ac sites (Bártfai et al., 2010). Similar to H3K9Ac, we find that PfGCN5 is mostly associated with the promoter regions of genes. Interestingly, the sites at which PfGCN5 and H3K9Ac bind do not follow an exact one-to-one correlation. This indicates that PfGCN5 may also have some functions in the parasite that are additional to histone acetylation. Indeed the GO analysis of genes recognized by PfGCN5 showed that they were involved in diverse physiological processes, such as transcription, entry into the host cell, cell differentiation and other biological processes. However,

these results may not reflect regulation of such genes by PfGCN5 solely due to its acetyl transferase activity on histones. Interestingly, in our MS results, we have found several non-histone proteins as possible PfGCN5 interacting partners (data not shown) suggesting multiple functions for this protein.

Notably, as shown in Fig. S1D, the multiple processed forms of PfGCN5 contain the C-terminal acetyltransferase domain. Thus, we can predict that acetylation function of PfGCN5 at those binding sites is active, possibly for histone H3 or some other protein substrates. Acetylation of non-histone substrates by GCN5 acetyltransferase has been reported in other systems (Dominy et al., 2012). However, this function is unexplored in malaria parasite.

Based on our findings, we propose a model depicting the possible events that happen during the processing of PfGCN5 protein on the vicinity of food vacuole before reaching the nucleus (Fig. 7). After synthesis of the full-length protein, it enters the ER-Golgi secretory pathway to reach the food vacuole of the parasite. Trafficking of the full-length protein at this step can be blocked by BFA treatment to the parasites. Furthermore, the full-length protein gets processed by a cysteine protease in the vicinity of the food vacuole. This processing is sensitive to well-known cysteine protease inhibitors E64d and MG132. At this moment, we lack evidence on nuclear import of these processed fragments. However, the subcellular fractionation and immunolocalization of the protein suggest processed PfGCN5 fragments indeed enter the nucleus. In the nucleus, PfGCN5 binds predominantly to the gene promoter regions, which is required either for its acetylation function on histone H3 or non-histone targets.

In conclusion, to our knowledge, this is the first report that suggests a direct role of a cysteine protease, most likely a food vacuole protease, in nuclear gene regulation in *Plasmodium*. Most notably, this is a constitutive function and is not dependent on any

cellular stress or other conditions, as observed in other organisms. Our results also emphasize the emerging role of *Plasmodium* ER-Golgi secretory pathway in processing of some nuclear proteins. Altogether, this study reveals new avenues on the regulation of the protein function in the malaria parasite and these could be employed as a key targets for generation of new antimalarial therapeutics.

MATERIALS AND METHODS

Reagents

Monoclonal antibody against H3K9Ac was a kind gift from Prof. Tapas Kumar Kundu, JNCASR, India. It was used at a dilution of 1:5000 for western blotting (WB), 1:3000 for the immunofluorescence assay (IFA) and 1:5000 for ChIP.

Antibodies against various *Plasmodium* proteins used in this study are as follows: PfActin (1:3000 for WB), PfAldolase (1:3000 for WB), PfSSB (1:3000 for WB), PfHsp70 (1:15,000 for WB) (made in house), PfBip (1:10,000 for WB, and 1:3000 for IFA; a kind gift from Prof. John Adams, University of Florida, FL).

The following antibodies were commercially purchased: antibodies against histone H3 (Ab1791, Abcam, 1:3000 for WB, 1.5 µg for ChIP), antibodies against GFP (G1544, Sigma-Aldrich, 1:5000 for WB), goat anti-mouse IgG conjugated to HRP (sc-2005, Santa Cruz Biotechnology, 1:5000 for WB), goat anti-rabbit IgG conjugated to HRP (sc-2004, Santa Cruz Biotechnology, 1:5000 for WB), Alexa Fluor® 488 (Ab150113 and Ab150077, Abcam, 1:500 for IFA), Alexa Fluor® 594 (Ab150080, Abcam, 1:500 for IFA) or Alexa Fluor® 568 (Ab175473, Abcam, 1:500 for IFA).

All inhibitors (E64d, MG132, epoxomicin and pepstatin A) used in this study were purchased from Sigma-Aldrich. Embelin was a kind gift from Prof. Tapas Kumar Kundu, JNCASR, India.

Parasite culture and synchronization

P. falciparum 3D7 parasites were cultured using standard protocols with slight modifications (Trager and Jensen, 1976). Briefly, the parasites

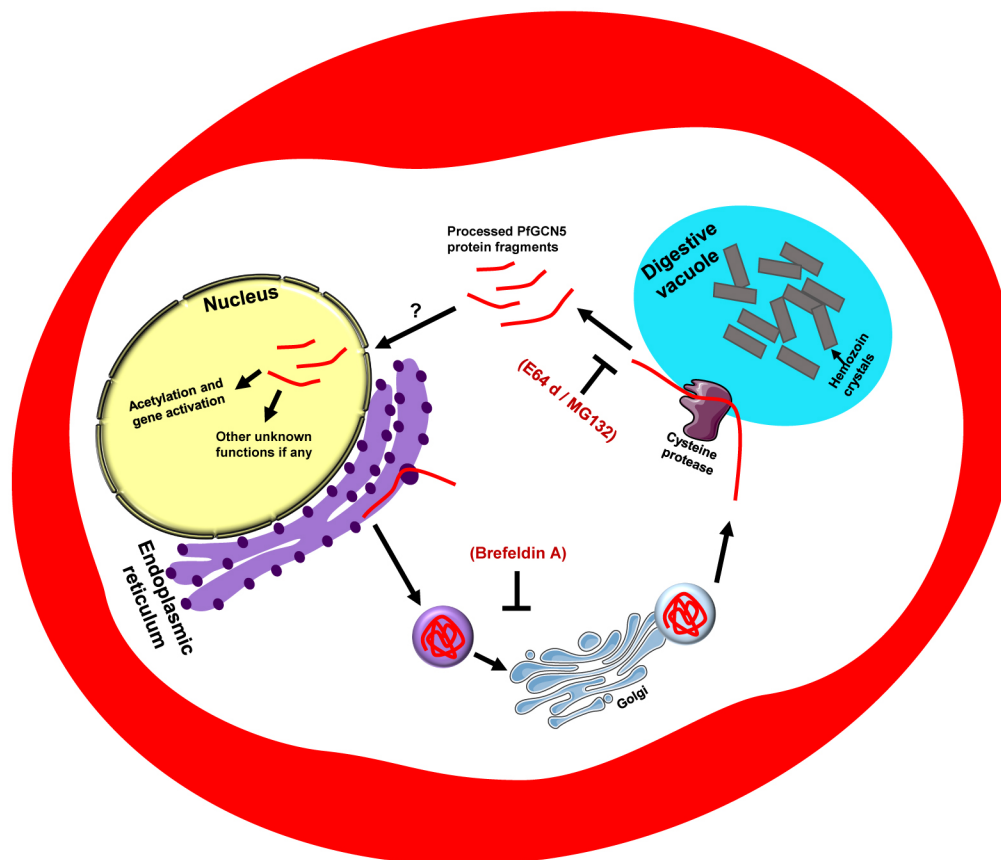


Fig. 7. Proposed model for the processing events of PfGCN5 in the parasite. The full-length PfGCN5 protein possibly gets translated on the ER and transports to the digestive vacuole via Golgi, in secretory vesicles. This ER-Golgi transport process can be blocked by brefeldin A (BFA). A cysteine protease that is either present on the food vacuole membrane or in close vicinity to the food vacuole processes the full-length protein in multiple specific fragments, all of which contain at least some of the C-terminal region of PfGCN5. These fragments enter the nucleus via an undefined route. In the parasite nucleus, these PfGCN5 fragments acetylate histone H3 or possibly some other proteins and regulate multiple cellular functions.

were cultivated in O⁺ human erythrocytes at 3% hematocrit in RPMI 1640 medium supplemented with 0.5% Albumax II (Invitrogen), 0.2% sodium bicarbonate (Sigma), 27.2 mg/l hypoxanthine (Sigma) and 50 mg/litre Gentamycin (Sigma). The parasites were grown at 37°C in an atmosphere of 5% CO₂, 5% O₂ and 90% nitrogen. Synchronization of parasites was carried out using 5% sorbitol treatment (Lambros and Vanderberg, 1979).

The parasite line overexpressing GFP-tagged PfAtg18 was generated by the laboratory of P.S.S. (CCMB). These parasites were also cultured using above protocol. Blasticidin S (0.5 µg/ml) was used for selection of these parasites. Western blotting using anti-GFP antibodies and live confocal images are shown in Fig. S5 for the confirmation of GFP-tagged PfAtg18 expression in the parasite.

Generation of polyclonal antibodies against PfGCN5

In order to generate specific antibodies against PfGCN5 (PF3d7_0823300) protein, the C-terminal domain of PfGCN5 (amino acids 1090–1463) was expressed and purified from *E. coli* as described previously (Kumar et al., 2017). Mice were immunized with recombinant His₆-PfGCN5 protein to generate the polyclonal anti-PfGCN5 antibodies following standard protocols. The specificity of the antibodies was determined through several experiments as described in results section. Dilutions of PfGCN5 for various experiments were as follows: 1:2500 for WB, 1:500 for IP, 1:500 for IFA and 1:500 for ChIP.

SDS-PAGE and western blot analysis

For immunoblotting, *P. falciparum*-infected RBCs were harvested and treated with 0.15% saponin for separation of parasites from RBC. Isolated parasites were further washed in 1× PBS solution containing protease inhibitor cocktail and resuspended in equal volume of 2× Laemmli SDS dye followed by boiling at 95°C for 4–5 min. After a brief centrifugation, total parasite protein extracts were separated from debris. In each lane, 40–60 µg of proteins were loaded and separated by SDS-PAGE. After that the proteins were transferred on polyvinylidenedifluoride (PVDF) membranes. The membranes were blocked by 5% skimmed milk in PBST (PBS with 0.1% Tween 20) followed by incubation with respective primary and HRP-conjugated secondary antibodies as applicable. The membranes were developed using the enhanced chemiluminescence solution. Densitometry analysis was performed using ImageJ software (NIH).

Immunoprecipitation and mass spectrometry analysis

Immunoprecipitation of PfGCN5 was carried out using Pierce Crosslink IP Kit from Thermo Fisher Scientific. Polyclonal antibodies against PfGCN5 were used to pull down the endogenous protein. Pre-immune PfGCN5 antibodies were used as a control. Following immunoprecipitation, proteins were eluted in the elution buffer provided in the kit. The eluted samples were processed for MS analysis using a previously described protocol (Gupta et al., 2018).

To analyze the multiple bands observed in western blot, the immunoprecipitated PfGCN5 sample was resolved in SDS-PAGE followed by silver staining using Bio-Rad Silver Stain Plus™ kit (catalog number: #161-0449). Respective gel bands were processed for MS analysis using previously described protocol (Gupta et al., 2018).

Subcellular fractionation

The subcellular fractionation of *P. falciparum* 3D7 parasites was performed using standard protocol (Flueck et al., 2009) with slight modifications. Saponin-lysed parasites were incubated on ice for 5 min in lysis buffer containing 20 mM HEPES pH 7.9, 10 mM KCl, 1 mM EGTA, 1 mM EDTA, 1 mM DTT, 0.65% NP-40, 100 µM PMSF and protease inhibitor cocktail. The supernatant containing cytoplasmic proteins was obtained by centrifugation at 865 g at 4°C. The pellet thus obtained was washed twice thoroughly with the above mentioned lysis buffer to remove any cytoplasmic contaminants. The nuclear fraction was finally obtained by centrifuging the sample at 865 g. Samples were prepared using SDS-PAGE loading buffer and equal amounts of sample from each fractions were resolved by SDS-PAGE and subjected to western blotting. Aldolase and histone were used as respective controls for cytoplasmic and nuclear fractions.

Na₂CO₃ extraction of parasite membrane proteins

Protein solubility was analyzed using a previously described procedure (Kulangara et al., 2012). The parasites were saponin-lysed and subjected to three freeze–thaw cycles in the presence of 5 mM Tris-HCl pH 8.0. Soluble protein fraction was obtained by high speed centrifugation at 16,249 g. The pellet so obtained was treated with 0.1 M Na₂CO₃ to extract peripheral membrane proteins. Next, integral membrane proteins were extracted using 1% Triton X-100. Subsequently the samples were centrifuged at high speed (16,249 g for 30 min) to recover pellet containing insoluble proteins. The insoluble fraction was resuspended in 2× SDS gel loading dye. The fractions so obtained were then subjected to SDS-PAGE and analyzed using immunoblotting with respective antibodies.

Immunofluorescence assay

The immunofluorescence assay was performed using protocols as described previously (Srivastava et al., 2014). After preparing the slides, they were scanned under Olympus confocal microscope. To analyze colocalization, Z-sectioning of selected images was performed followed by 3D reconstruction of images using Olympus FV31S-SW software. Pearson correlation coefficient values are given in the results to signify the colocalization between two proteins. Antibodies used for IFA and their dilutions are given in the reagents section.

Immuno-electron microscopy

Immuno-EM was performed using the method described previously (Sharma et al., 2018). All the steps were performed at 4°C or as otherwise mentioned. Briefly, mixed stage parasite-infected erythrocytes were fixed overnight using a mixture of 0.1% glutaraldehyde and 4% paraformaldehyde. Graded alcohol dehydrations (30%, 50%, 70%, 80% and 90%) were then performed for 30 min each, followed by two absolute alcohol dehydrations for 1 h. The parasites were then infiltrated using a 1:1 solution of LR White and absolute alcohol twice for 1 h each. Further infiltration was performed overnight by using only LR White and next day again at room temperature for 4 h. Finally, embedding was carried out at 55°C for 48 h after adding 5 volumes of LR White to the pellet. Ultra-thin sections were subsequently cut and incubated with anti-PfGCN5 primary antibodies at a dilution of 1:10 followed by secondary antibodies that were conjugated to 10 nm gold particles. The immuno-labeled samples were then examined using JEOL JEM-F200 electron microscope at IUAC, New Delhi.

Isolation of parasite food vacuole

Purification of food vacuole was performed from MG132-treated parasites following a protocol described elsewhere (Saliba et al., 1998). Briefly, late-stage parasites were treated with 100 nM MG132 for 4 h. Parasites were released from RBCs after saponin treatment followed by lysis of parasites in ice cold water (pH 4.5) and trituration through 27G needle. After that sample was treated with DNase I. Following centrifugation, the pellet was resuspended in ice cold 42% Percoll solution containing 0.25 M sucrose, 1.25 mM MgSO₄. Finally, the sample was centrifuged at 18,845 g for 10 min and food vacuole was collected as pellet.

ChIP and next-generation sequencing

Asynchronous stage parasites (trophozoite and schizont enriched) with 10% parasitemia were harvested and fixed with 1% formaldehyde at 37°C for 10 min. To prevent the over crosslinking, excess formaldehyde was quenched by addition of glycine to a final concentration of 150 mM. After that, the parasitized RBCs were washed twice with 1× PBS followed by saponin lysis to remove the RBCs. Then the parasites were resuspended in ice-cold SDS lysis buffer (1% SDS, 10 mM EDTA, 50 mM Tris-HCl, pH 8.1) supplemented with PMSF (100 µM) and protease inhibitor cocktail (Roche) for 10 min on ice. Parasite lysate was then sonicated to generate sheared chromatin of ~500 bp fragments and centrifuged at 1000 g for 15 min. After the removal of debris from the lysate, the lysate was further diluted 10 times in ChIP dilution buffer (0.01% SDS, 0.1% Triton-X 100, 1.2 mM EDTA, 16.7 mM Tris-HCl pH 8.1, and 150 mM NaCl). Subsequently, the parasite lysates were precleared using protein A–sepharose beads at 4°C for 1 h. Cleared chromatin was incubated

with pre-immune sera and immune GCN5 sera for overnight at 4°C on a rotating wheel. The formed chromatin immunocomplexes were precipitated with protein A–sepharose beads. The beads were washed for 5 min at 4°C with low-salt wash buffer (0.1% SDS, 1% Triton X-100, 2 mM EDTA, 20 mM Tris-HCl, pH 8.1, 150 mM NaCl), high-salt wash buffer (0.1% SDS, 1% Triton X-100, 2 mM EDTA, 20 mM Tris-HCl, pH 8.1, 500 mM NaCl), LiCl wash buffer [0.25 M LiCl, 1% IGEPAL-CA630, 1% deoxycholic acid (sodium salt), 1 mM EDTA, 10 mM Tris-HCl pH 8.1] and TE buffer (10 mM Tris-HCl, 1 mM EDTA, pH 8.0). The DNA–protein complex was eluted using 500 µl of freshly prepared elution buffer (1% SDS, 0.1 M NaHCO₃) followed by de-crosslinking with NaCl (300 mM final concentration) at 65°C for overnight. After de-crosslinking the samples were further treated with proteinase K (20 µg/ml) at 45°C for 1 h. Finally, the DNA was isolated by phenol-chloroform extraction and dissolved in TE buffer for sequencing or quantitative PCR analysis.

ChIP-sequencing was carried out at Xcelris Labs Ltd, Ahmedabad. Briefly, the paired-end sequencing library was prepared using IlluminaTruSeqNano DNA LT Library Preparation Kit following manufacturer's instructions. After obtaining the concentration for the library and the mean peak size from Bioanalyser profile, the library was loaded onto Illumina platform for cluster generation and sequencing. The generated fastq files were further analyzed and described below.

Next generation sequencing data analysis

The high quality paired end ChIP-seq reads generated through hi-throughput sequencing were mapped with the reference genome (PlasmoDB-41_Pfalciparum 3D7) using Bowtie2 (v2.1.0). We further carried out conversion of SAM files to BAM and sorting with Samtools (v0.1.19) followed by removing duplicate reads using Picard. In order to get an idea about the binding loci of the GCN5 in the genome, we carried out method for peak calling using MACS2 (v2.1.2) with a 0.05 *P*-value cutoff. The identified loci in the first step were annotated in terms of genomic (PlasmoDB-39_Pfalciparum 3D7) context using Homer. Visualization of binding location in the reference genome we have done using IGV (v2.4.16) and the coverage plot has been done with ChIPseeker library in R. The genes in the vicinity or nearby regions were taken for Gene Ontology (GO) enrichment and pathway analysis. In addition, we have downloaded the invasion genes from PlasmoDB database to see its abundance around the GCN5 genomic region. We have downloaded high quality H3K9ac ChIP-seq reads from GEO-NCBI (GSM588517, GSM588518, GSM588525 and GSM588526) for further analysis. To validate and improve the confidence level of data generation we have mapped and compare the loci of H3K9ac (trophozoite and schizont stage) with GCN5 ChIP-seq data; this helps us to get an idea about the relatedness of the binding patterns.

ChIP-quantitative PCR analysis

To validate the results obtained from ChIP-seq analysis, we chose several low-to-high PfGCN5-binding regions for ChIP followed by quantitative PCR (qPCR) analysis. Primers used for quantitative PCR were listed in Table S2. ChIP samples were prepared using anti-PfGCN5 antibodies following protocol described above. Quantitative PCR was performed with specific primers, using Luna[®] Universal qPCR solution (NEB). The Ct values were used for further calculations and plotted in bar diagram.

Acknowledgements

The authors acknowledge Dr Debdulal Kabiraj and Electron Microscopy facility at IUAC, Delhi for the help with Electron Microscopy. Prof. Tapas Kumar Kundu, JNCASR, Bangalore, India is acknowledged for providing antibodies against H3K9Ac.

Competing interests

The authors declare no competing or financial interests.

Author contributions

Conceptualization: K.B.; Methodology: K.B., S.V., I.K., A.K., S.K.D.; Validation: K.B., A.T.; Formal analysis: K.B., A.T., S.V., R.S., I.K., P.S.S., A.K., S.K.D.; Investigation: K.B., A.T., S.V., R.S.; Resources: I.K., P.S.S., A.K., S.K.D.; Data curation: K.B., A.T., S.V.; Writing - original draft: K.B.; Writing - review & editing: K.B., A.T., S.V., P.S.S., A.K., S.K.D.; Visualization: K.B.; Supervision: K.B., P.S.S., A.K., S.K.D.; Funding acquisition: S.K.D.

Funding

The authors acknowledge Department of Biotechnology, Ministry of Science and Technology (BT/PR15639/MED/29/1145/2016), Department of Science and Technology (DST-PURSE) and the University Grants Commission (UGC-SAP) for funding. K.B. acknowledges UGC, A.T. acknowledges CSIR, Renu acknowledges DBT and Sunita acknowledges UGC, India for fellowships.

Data availability

ChIP-seq data from this study has been deposited in the Gene Expression Omnibus (GEO) under accession no. GSE142803.

Supplementary information

Supplementary information available online at <http://jcs.biologists.org/lookup/doi/10.1242/jcs.236489.supplemental>

References

- Agbor-Enoh, S., Seudieu, C., Davidson, E., Dritschilo, A. and Jung, M. (2009). Novel inhibitor of Plasmodium histone deacetylase that cures *P. berghei*-infected mice. *Antimicrob. Agents Chemother.* **53**, 1727-1734. doi:10.1128/AAC.00729-08
- Bansal, P., Tripathi, A., Thakur, V., Mohammed, A. and Sharma, P. (2017). Autophagy-related protein ATG18 regulates apicoplast biogenesis in apicomplexan parasites. *MBio* **8**, e01468-17. doi:10.1128/mBio.01468-17
- Barber, B. E., Rajahram, G. S., Grigg, M. J., William, T. and Anstey, N. M. (2017). World malaria report: time to acknowledge Plasmodium knowlesi malaria. *Malar. J.* **16**, 135. doi:10.1186/s12936-017-1787-y
- Bártfai, R., Hoeijmakers, W. A., Salcedo-Amaya, A. M., Smits, A. H., Janssen-Megens, E., Kaan, A., Treeck, M., Gilberger, T. W., Francoijs, K. J. and Stunnenberg, H. G. (2010). H2A.Z demarcates intergenic regions of the plasmodium falciparum epigenome that are dynamically marked by H3K9ac and H3K4me3. *PLoS Pathog.* **6**, e1001223. doi:10.1371/journal.ppat.1001223
- Benting, J., Mattei, D. and Lingelbach, K. (1994). Brefeldin A inhibits transport of the glycoporphin-binding protein from Plasmodium falciparum into the host erythrocyte. *Biochem. J.* **300**, 821-826. doi:10.1042/bj3000821
- Bhatti, M. M. and Sullivan, W. J. Jr. (2005). Histone acetylase GCN5 enters the nucleus via importin-alpha in protozoan parasite Toxoplasma gondii. *J. Biol. Chem.* **280**, 5902-5908. doi:10.1074/jbc.M410656200
- Bhatti, M. M., Livingston, M., Mullanpudi, N. and Sullivan, W. J. Jr. (2006). Pair of unusual GCN5 histone acetyltransferases and ADA2 homologues in the protozoan parasite Toxoplasma gondii. *Eukaryot. Cell* **5**, 62-76. doi:10.1128/EC.5.1.62-76.2006
- Blackman, M. J., Ling, I. T., Nicholls, S. C. and Holder, A. A. (1991). Proteolytic processing of the Plasmodium falciparum merozoite surface protein-1 produces a membrane-bound fragment containing two epidermal growth factor-like domains. *Mol. Biochem. Parasitol.* **49**, 29-33. doi:10.1016/0166-6851(91)90127-R
- Brownell, J. E. and Allis, C. D. (1995). An activity gel assay detects a single, catalytically active histone acetyltransferase subunit in Tetrahymena macronuclei. *Proc. Natl. Acad. Sci. USA* **92**, 6364-6368. doi:10.1073/pnas.92.14.6364
- Brownell, J. E., Zhou, J., Ranalli, T., Kobayashi, R., Edmondson, D. G., Roth, S. Y. and Allis, C. D. (1996). Tetrahymena histone acetyltransferase A: a homolog to yeast Gcn5p linking histone acetylation to gene activation. *Cell* **84**, 843-851. doi:10.1016/S0092-8674(00)81063-6
- Bushell, E., Gomes, A. R., Sanderson, T., Anar, B., Girling, G., Herd, C., Metcalf, T., Modrzynska, K., Schwach, F., Martin, R. E. et al. (2017). Functional profiling of a plasmodium genome reveals an abundance of essential genes. *Cell* **170**, 260-272.e8. doi:10.1016/j.cell.2017.06.030
- Carrozza, M. J., Utley, R. T., Workman, J. L. and Cote, J. (2003). The diverse functions of histone acetyltransferase complexes. *Trends Genet.* **19**, 321-329. doi:10.1016/S0168-9525(03)00115-X
- Chua, M. J., Arnold, M. S., Xu, W., Lancelot, J., Lamotte, S., Spath, G. F., Prina, E., Pierce, R. J., Fairlie, D. P., Skinner-Adams, T. S. et al. (2017). Effect of clinically approved HDAC inhibitors on Plasmodium, Leishmania and Schistosoma parasite growth. *Int. J. Parasitol. Drugs Drug Resist.* **7**, 42-50. doi:10.1016/j.ijpddr.2016.12.005
- Croken, M. M., Nardelli, S. C. and Kim, K. (2012). Chromatin modifications, epigenetics, and how protozoan parasites regulate their lives. *Trends Parasitol.* **28**, 202-213. doi:10.1016/j.pt.2012.02.009
- Cui, L., Miao, J., Furuya, T., Li, X. and Su, X. Z. (2007). PfGCN5-mediated histone H3 acetylation plays a key role in gene expression in Plasmodium falciparum. *Eukaryot. Cell* **6**, 1219-1227. doi:10.1128/EC.00062-07
- Dominy, J. E., Jr., Lee, Y., Jedrychowski, M. P., Chim, H., Jurczak, M. J., Camporez, J. P., Ruan, H. B., Feldman, J., Pierce, K., Mostoslavsky, R. et al. (2012). The deacetylase Sirt6 activates the acetyltransferase GCN5 and suppresses hepatic gluconeogenesis. *Mol. Cell* **48**, 900-913. doi:10.1016/j.molcel.2012.09.030
- Fan, Q., An, L. and Cui, L. (2004a). PfADA2, a Plasmodium falciparum homologue of the transcriptional coactivator ADA2 and its in vivo association with the histone acetyltransferase PfGCN5. *Gene* **336**, 251-261. doi:10.1016/j.gene.2004.04.005

- Fan, Q., An, L. and Cui, L. (2004b). Plasmodium falciparum histone acetyltransferase, a yeast GCN5 homologue involved in chromatin remodeling. *Eukaryot. Cell* **3**, 264-276. doi:10.1128/EC.3.2.264-276.2004
- Flueck, C., Bártfai, R., Volz, J., Niederwieser, I., Salcedo-Amaya, A. M., Alako, B. T. F., Ehlgren, F., Ralph, S. A., Cowman, A. F., Bozdech, Z. et al. (2009). Plasmodium falciparum heterochromatin protein 1 marks genomic loci linked to phenotypic variation of exported virulence factors. *PLoS Pathog.* **5**, e1000569. doi:10.1371/journal.ppat.1000569
- Foth, B. J., Zhang, N., Chaal, B. K., Sze, S. K., Preiser, P. R. and Bozdech, Z. (2011). Quantitative time-course profiling of parasite and host cell proteins in the human malaria parasite Plasmodium falciparum. *Mol. Cell. Proteomics* **10**, M110.006411. doi:10.1074/mcp.M110.006411
- Fournier, M., Orpinell, M., Grauffel, C., Scheer, E., Garnier, J. M., Ye, T., Chavant, V., Joint, M., Esashi, F., Dejaegere, A. et al. (2016). KAT2A/KAT2B-targeted acetylation reveals a role for PLK4 acetylation in preventing centrosome amplification. *Nat. Commun.* **7**, 13227. doi:10.1038/ncomms13227
- Gao, B., Kong, Q., Zhang, Y., Yun, C., Dent, S. Y. R., Song, J., Zhang, D. D., Wang, Y., Li, X. and Fang, D. (2017). The histone acetyltransferase Gcn5 positively regulates T cell activation. *J. Immunol.* **198**, 3927-3938. doi:10.4049/jimmunol.1600312
- Gates, L. A., Shi, J., Rohira, A. D., Feng, Q., Zhu, B., Bedford, M. T., Sagum, C. A., Jung, S. Y., Qin, J., Tsai, M. J. et al. (2017). Acetylation on histone H3 lysine 9 mediates a switch from transcription initiation to elongation. *J. Biol. Chem.* **292**, 14456-14472. doi:10.1074/jbc.M117.802074
- Grant, P. A., Duggan, L., Cote, J., Roberts, S. M., Brownell, J. E., Candau, R., Ohba, R., Owen-Hughes, T., Allis, C. D., Winston, F. et al. (1997). Yeast Gcn5 functions in two multisubunit complexes to acetylate nucleosomal histones: characterization of an Ada complex and the SAGA (Spt/Ada) complex. *Genes Dev.* **11**, 1640-1650. doi:10.1101/gad.11.13.1640
- Grant, P. A., Eberharter, A., John, S., Cook, R. G., Turner, B. M. and Workman, J. L. (1999). Expanded lysine acetylation specificity of Gcn5 in native complexes. *J. Biol. Chem.* **274**, 5895-5900. doi:10.1074/jbc.274.9.5895
- Gupta, M. K., Agarawal, M., Banu, K., Reddy, K. S., Gaur, D. and Dhar, S. K. (2018). Role of Chromatin assembly factor 1 in DNA replication of Plasmodium falciparum. *Biochem. Biophys. Res. Commun.* **495**, 1285-1291. doi:10.1016/j.bbrc.2017.11.131
- Herrera-Solorio, A. M., Vembar, S. S., MacPherson, C. R., Lozano-Amado, D., Meza, G. R., Xocostle-Cazares, B., Martins, R. M., Chen, P., Vargas, M., Scherf, A. et al. (2019). Clipped histone H3 is integrated into nucleosomes of DNA replication genes in the human malaria parasite Plasmodium falciparum. *EMBO Rep.* **20**, e46331. doi:10.15252/embr.201846331
- Joice, R., Narasimhan, V., Montgomery, J., Sidhu, A. B., Oh, K., Meyer, E., Pierre-Louis, W., Seydel, K., Milner, D., Williamson, K. et al. (2013). Inferring developmental stage composition from gene expression in human malaria. *PLoS Comput. Biol.* **9**, e1003392. doi:10.1371/journal.pcbi.1003392
- Karmodiya, K., Pradhan, S. J., Joshi, B., Jangid, R., Reddy, P. C. and Galande, S. (2015). A comprehensive epigenome map of Plasmodium falciparum reveals unique mechanisms of transcriptional regulation and identifies H3K36me2 as a global mark of gene suppression. *Epigenetics Chromatin* **8**, 32. doi:10.1186/s13072-015-0029-1
- Kelly, T. J., Lerin, C., Haas, W., Gygi, S. P. and Puigserver, P. (2009). GCN5-mediated transcriptional control of the metabolic coactivator PGC-1 β through lysine acetylation. *J. Biol. Chem.* **284**, 19945-19952. doi:10.1074/jbc.M109.015164
- Kikuchi, H., Kuribayashi, F., Takami, Y., Imajoh-Ohmi, S. and Nakayama, T. (2011). GCN5 regulates the activation of PI3K/Akt survival pathway in B cells exposed to oxidative stress via controlling gene expressions of Syk and Btk. *Biochem. Biophys. Res. Commun.* **405**, 657-661. doi:10.1016/j.bbrc.2011.01.088
- Kirchner, S., Power, B. J. and Waters, A. P. (2016). Recent advances in malaria genomics and epigenomics. *Genome Med.* **8**, 92. doi:10.1186/s13073-016-0343-7
- Klemba, M., Beatty, W., Gluzman, I. and Goldberg, D. E. (2004). Trafficking of plasmepsin II to the food vacuole of the malaria parasite Plasmodium falciparum. *J. Cell Biol.* **164**, 47-56. doi:10.1083/jcb.200307147
- Kuhn, Y., Sanchez, C. P., Ayoub, D., Saridaki, T., van Dorselaer, A. and Lanzer, M. (2010). Trafficking of the phosphoprotein PfCRT to the digestive vacuolar membrane in Plasmodium falciparum. *Traffic* **11**, 236-249. doi:10.1111/j.1600-0854.2009.01018.x
- Kulangara, C., Luedin, S., Dietz, O., Rusch, S., Frank, G., Mueller, D., Moser, M., Kajava, A. V., Corradin, G., Beck, H. P. et al. (2012). Cell biological characterization of the malaria vaccine candidate trophozoite exported protein 1. *PLoS ONE* **7**, e46112. doi:10.1371/journal.pone.0046112
- Kumar, A., Bhowmick, K., Vikramdeo, K. S., Mondal, N., Subbarao, N. and Dhar, S. K. (2017). Designing novel inhibitors against histone acetyltransferase (HAT: GCN5) of Plasmodium falciparum. *Eur. J. Med. Chem.* **138**, 26-37. doi:10.1016/j.ejmech.2017.06.009
- Lambros, C. and Vanderberg, J. P. (1979). Synchronization of Plasmodium falciparum erythrocytic stages in culture. *J. Parasitol.* **65**, 418-420. doi:10.2307/3280287
- Lerin, C., Rodgers, J. T., Kalume, D. E., Kim, S. H., Pandey, A. and Puigserver, P. (2006). GCN5 acetyltransferase complex controls glucose metabolism through transcriptional repression of PGC-1 α . *Cell Metab.* **3**, 429-438. doi:10.1016/j.cmet.2006.04.013
- Lee, D.H. and Goldberg, A.L. (1998). Proteasome inhibitors: valuable new tools for cell biologists. *Trends Cell Biol.* **8**, 397-403. doi:10.1016/s0962-8924(98)01346-4
- Le Roch, K. G., Johnson, J. R., Florens, L., Zhou, Y., Santrosyan, A., Grainger, M., Yan, S. F., Williamson, K. C., Holder, A. A., Carucci, D. J. et al. (2004). Global analysis of transcript and protein levels across the Plasmodium falciparum life cycle. *Genome Res.* **14**, 2308-2318. doi:10.1101/gr.2523904
- Lin, C. S., Uboldi, A. D., Epp, C., Bujard, H., Tsuboi, T., Czabotar, P. E. and Cowman, A. F. (2016). Multiple plasmodium falciparum merozoite surface protein 1 complexes mediate merozoite binding to human erythrocytes. *J. Biol. Chem.* **291**, 7703-7715. doi:10.1074/jbc.M115.698282
- Liu, Y., Li, P., Fan, L. and Wu, M. (2018). The nuclear transportation routes of membrane-bound transcription factors. *Cell Commun. Signal* **16**, 12. doi:10.1186/s12964-018-0224-3
- Malmquist, N. A., Moss, T. A., Mecheri, S., Scherf, A. and Fuchter, M. J. (2012). Small-molecule histone methyltransferase inhibitors display rapid antimalarial activity against all blood stage forms in Plasmodium falciparum. *Proc. Natl. Acad. Sci. USA* **109**, 16708-16713. doi:10.1073/pnas.1205414109
- Meng, L., Mohan, R., Kwok, B. H. B., Elofsson, M., Sin, N. and Crews, C. M. (1999). Epoxomicin, a potent and selective proteasome inhibitor, exhibits in vivo anti-inflammatory activity. *Proc. Natl. Acad. Sci. USA* **96**, 10403-10408. doi:10.1073/pnas.96.18.10403
- Merrick, C. J., Huttenhower, C., Buckee, C., Amambua-Ngwa, A., Gomez-Escobar, N., Walther, M., Conway, D. J. and Duraisingh, M. T. (2012). Epigenetic dysregulation of virulence gene expression in severe Plasmodium falciparum malaria. *J. Infect. Dis.* **205**, 1593-1600. doi:10.1093/infdis/jis239
- Orpinell, M., Fournier, M., Riss, A., Nagy, Z., Krebs, A. R., Frontini, M. and Toral, L. (2010). The ATAC acetyl transferase complex controls mitotic progression by targeting non-histone substrates. *EMBO J.* **29**, 2381-2394. doi:10.1038/emboj.2010.125
- Painter, H. J., Carrasquilla, M. and Linás, M. (2017). Capturing in vivo RNA transcriptional dynamics from the malaria parasite Plasmodium falciparum. *Genome Res.* **27**, 1074-1086. doi:10.1101/gr.217356.116
- Paolinelli, R., Mendoza-Maldonado, R., Cereseto, A. and Giacca, M. (2009). Acetylation by GCN5 regulates CDC6 phosphorylation in the S phase of the cell cycle. *Nat. Struct. Mol. Biol.* **16**, 412-420. doi:10.1038/nsmb.1583
- Phan, H. M., Xu, A. W., Coco, C., Srajer, G., Wyszomierski, S., Evrard, Y. A., Eckner, R. and Dent, S. Y. (2005). GCN5 and p300 share essential functions during early embryogenesis. *Dev. Dyn.* **233**, 1337-1347. doi:10.1002/dvdy.20445
- Pokholok, D. K., Harbison, C. T., Levine, S., Cole, M., Hannett, N. M., Lee, T. I., Bell, G. W., Walker, K., Rolfe, P. A., Herbolsheimer, E. et al. (2005). Genome-wide map of nucleosome acetylation and methylation in yeast. *Cell* **122**, 517-527. doi:10.1016/j.cell.2005.06.026
- Prasad, R., Atul, Kolla, V. K., Legac, J., Singhal, N., Navale, R., Rosenthal, P. J. and Sijwali, P. S. (2013). Blocking Plasmodium falciparum development via dual inhibition of hemoglobin degradation and the ubiquitin proteasome system by MG132. *PLoS ONE* **8**, e73530. doi:10.1371/journal.pone.0073530
- Salcedo-Amaya, A. M., van Driel, M. A., Alako, B. T., Trelle, M. B., van den Elzen, A. M., Cohen, A. M., Janssen-Megens, E. M., van de Vegte-Bolmer, M., Selzer, R. R., Iniguez, A. L. et al. (2009). Dynamic histone H3 epigenome marking during the intraerythrocytic cycle of Plasmodium falciparum. *Proc. Natl. Acad. Sci. USA* **106**, 9655-9660. doi:10.1073/pnas.0902515106
- Saliba, K. J., Folb, P. I. and Smith, P. J. (1998). Role for the plasmodium falciparum digestive vacuole in chloroquine resistance. *Biochem. Pharmacol.* **56**, 313-320. doi:10.1016/S0006-2952(98)00140-3
- Sharma, R., Sharma, B., Gupta, A. and Dhar, S. K. (2018). Identification of a novel trafficking pathway exporting a replication protein, Orc2 to nucleus via classical secretory pathway in Plasmodium falciparum. *Biochim. Biophys. Acta Mol. Cell Res.* **1865**, 817-829. doi:10.1016/j.bbamcr.2018.03.003
- Sijwali, P. S., Koo, J., Singh, N. and Rosenthal, P. J. (2006). Gene disruptions demonstrate independent roles for the four falcipain cysteine proteases of Plasmodium falciparum. *Mol. Biochem. Parasitol.* **150**, 96-106. doi:10.1016/j.molbiopara.2006.06.013
- Siqueira-Neto, J. L., Debnath, A., McCall, L. I., Bernatchez, J. A., Ndao, M., Reed, S. L. and Rosenthal, P. J. (2018). Cysteine proteases in protozoan parasites. *PLoS Negl. Trop. Dis.* **12**, e0006512. doi:10.1371/journal.pntd.0006512
- Skvirsky, R. C., Greenberg, M. L., Myers, P. L. and Greer, H. (1986). A new negative control gene for amino acid biosynthesis in Saccharomyces cerevisiae. *Curr. Genet.* **10**, 495-501. doi:10.1007/BF00447382
- Smith, E. R., Belote, J. M., Schiltz, R. L., Yang, X. J., Moore, P. A., Berger, S. L., Nakatani, Y. and Allis, C. D. (1998). Cloning of Drosophila GCN5: conserved features among metazoan GCN5 family members. *Nucleic Acids Res.* **26**, 2948-2954. doi:10.1093/nar/26.12.2948
- Srivastava, S., Bhowmick, K., Chatterjee, S., Basha, J., Kundu, T. K. and Dhar, S. K. (2014). Histone H3K9 acetylation level modulates gene expression and may affect parasite growth in human malaria parasite Plasmodium falciparum. *FEBS J.* **281**, 5265-5278. doi:10.1111/febs.13067
- Subramanian, S., Sijwali, P. S. and Rosenthal, P. J. (2007). Falcipain cysteine proteases require bipartite motifs for trafficking to the Plasmodium falciparum food vacuole. *J. Biol. Chem.* **282**, 24961-24969. doi:10.1074/jbc.M703316200

- Tonkin, C. J., Struck, N. S., Mullin, K. A., Stimmler, L. M. and McFadden, G. I.** (2006). Evidence for Golgi-independent transport from the early secretory pathway to the plastid in malaria parasites. *Mol. Microbiol.* **61**, 614-630. doi:10.1111/j.1365-2958.2006.05244.x
- Trager, W. and Jensen, J. B.** (1976). Human malaria parasites in continuous culture. *Science* **193**, 673-675. doi:10.1126/science.781840
- Trisciuglio, D., Di Martile, M. and Del Bufalo, D.** (2018). Emerging role of histone acetyltransferase in stem cells and cancer. *Stem Cells Int.* **2018**, 8908751. doi:10.1155/2018/8908751
- Wang, Z., Zang, C., Rosenfeld, J. A., Schones, D. E., Barski, A., Cuddapah, S., Cui, K., Roh, T. Y., Peng, W., Zhang, M. Q. et al.** (2008). Combinatorial patterns of histone acetylations and methylations in the human genome. *Nat. Genet.* **40**, 897-903. doi:10.1038/ng.154
- Wang, Y., Miao, X., Liu, Y., Li, F., Liu, Q., Sun, J. and Cai, L.** (2014). Dysregulation of histone acetyltransferases and deacetylases in cardiovascular diseases. *Oxid. Med. Cell. Longev.* **2014**, 641979. doi:10.1155/2014/641979
- Xiao, B., Yin, S., Hu, Y., Sun, M., Wei, J., Huang, Z., Wen, Y., Dai, X., Chen, H., Mu, J. et al.** (2019). Epigenetic editing by CRISPR/dCas9 in *Plasmodium falciparum*. *Proc. Natl. Acad. Sci. USA* **116**, 255-260. doi:10.1073/pnas.1813542116
- Xu, W., Edmondson, D. G. and Roth, S. Y.** (1998). Mammalian GCN5 and P/CAF acetyltransferases have homologous amino-terminal domains important for recognition of nucleosomal substrates. *Mol. Cell. Biol.* **18**, 5659-5669. doi:10.1128/MCB.18.10.5659
- Zhang, M., Wang, C., Otto, T. D., Oberstaller, J., Liao, X., Adapa, S. R., Udenze, K., Bronner, I. F., Casandra, D., Mayho, M. et al.** (2018). Uncovering the essential genes of the human malaria parasite *Plasmodium falciparum* by saturation mutagenesis. *Science* **360**, eaap7847. doi:10.1126/science.aap7847
- Zhou, J., Wang, X., He, K., Charron, J.-B., Elling, A. A. and Deng, X. W.** (2010). Genome-wide profiling of histone H3 lysine 9 acetylation and dimethylation in *Arabidopsis* reveals correlation between multiple histone marks and gene expression. *Plant Mol. Biol.* **72**, 585-595. doi:10.1007/s11103-009-9594-7

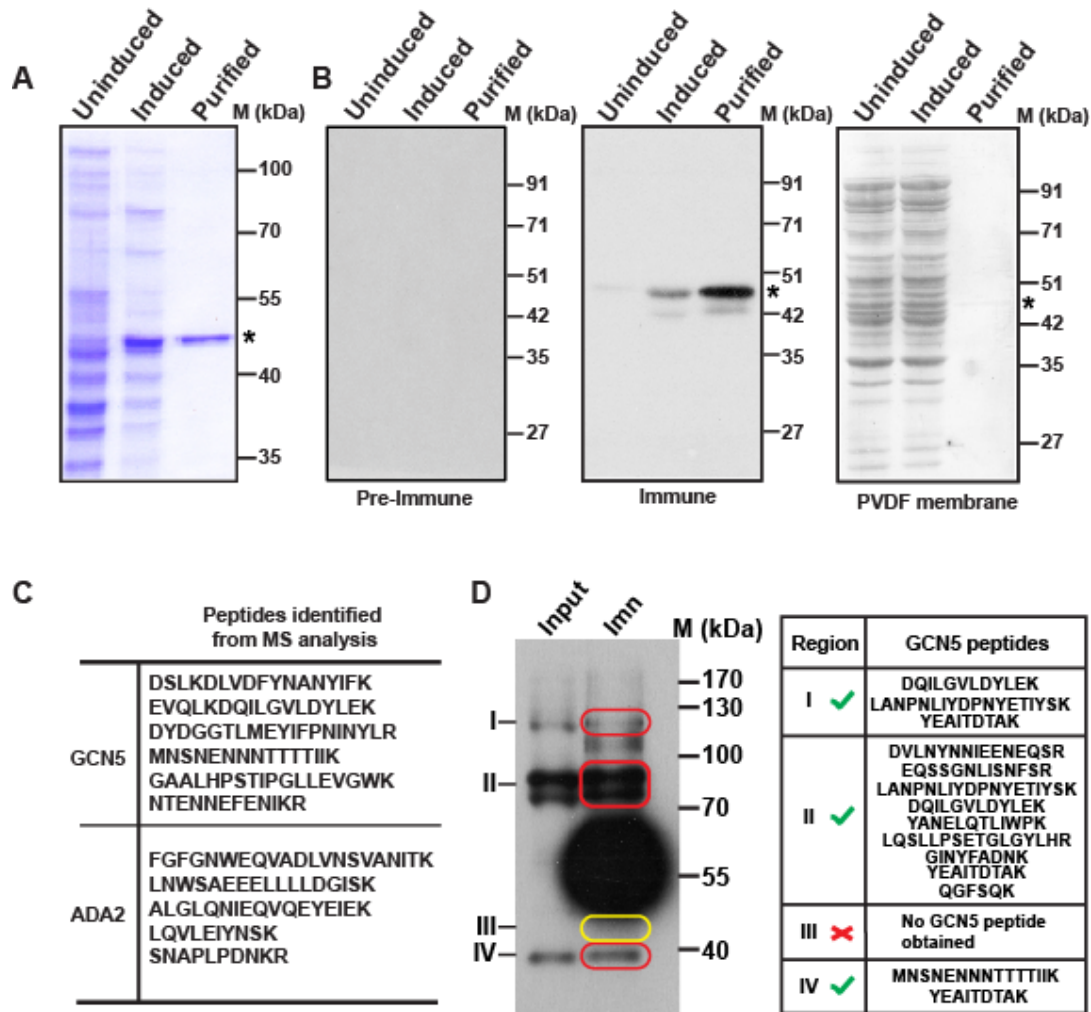


Figure S1. Specificity of mouse polyclonal antibodies generated against PfGCN5 protein and Mass spectrometric analysis of different bands corresponding to PfGCN5. (A) Coomassie stained gel showing purification profile of recombinant His₆-PfGCN5 protein. ‘*’ indicates the purified protein band that is also present in the lane corresponding to induced bacterial cell lysate. (B) Western blot analysis of purified PfGCN5 protein using pre-immune (left blot) and immune PfGCN5 sera (middle blot). Coomassie stained PVDF membrane after protein transfer on the right indicates the presence of protein in each lane. ‘*’ indicates the purified protein band. (C) List of peptides identified from in solution MS analysis of GCN5-IP sample corresponding to PfGCN5 and PfADA2. (D) Western blot analysis of Immunoprecipitated PfGCN5 from *P. falciparum* lysate using antibodies against PfGCN5. The IP sample was also subjected to SDS-PAGE under similar experimental conditions followed by silver staining (data not shown). Regions (I to IV) as indicated in immune IP lane were excised from silver stained gel and subjected to MS analysis. List of peptides detected in MS analysis corresponding to regions I, II and IV is shown on the right suggesting that the bands detected by anti-PfGCN5 sera are generated from full-length PfGCN5 protein.



Figure S2. Accumulation of ubiquitinated proteins in epoxomicin treated parasite. Parasites were treated with DMSO and epoxomicin separately followed by Western blot analysis using antibodies against ubiquitin.

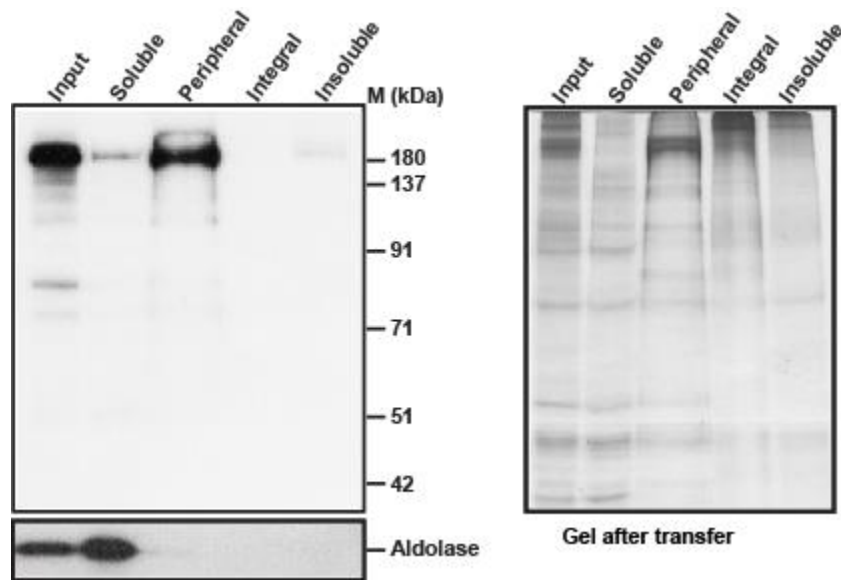


Figure S3. The full-length PfGCN5 protein is a peripheral membrane associated protein. To check the membrane association of full-length PfGCN5 protein, MG132 treated parasites were fractionated using protocol described in materials and methods. Equal amount of sample from each fraction was subjected for Western blot analysis. PfGCN5 is predominantly extracted in sodium carbonate extractable fraction (left panel) confirming its association with the peripheral membrane. Coomassie stained gel after transfer on right shows the similar loading of proteins from each fraction.

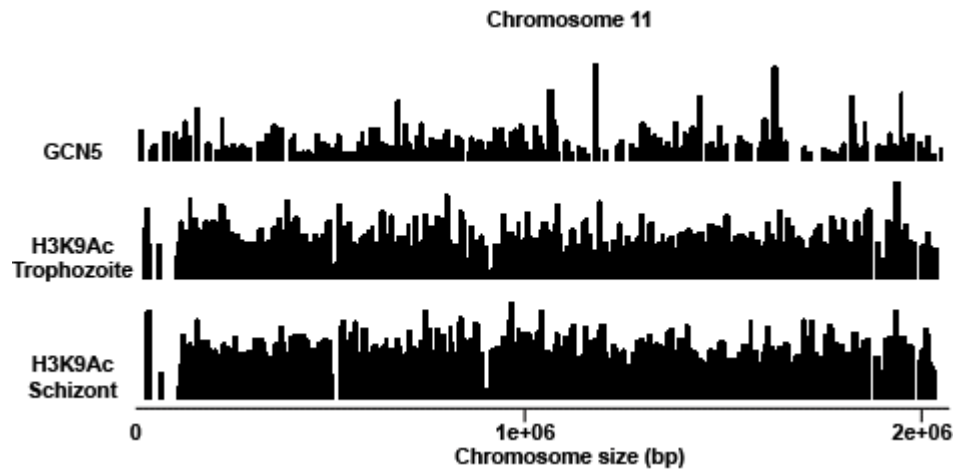


Figure S4. Comparative alignment of GCN5, H3K9Ac (trophozoite stage) and H3K9Ac (Schizont stage) ChIP-seq coverage plots. Upper panel shows the PfGCN5 binding sites on chromosome 11. PfGCN5 ChIP-sequencing was performed in asynchronous stages parasites. PfH3K9Ac ChIP-sequencing results were obtained from Bartfai et al., 2010. Chromosome size (bp) is indicated below.

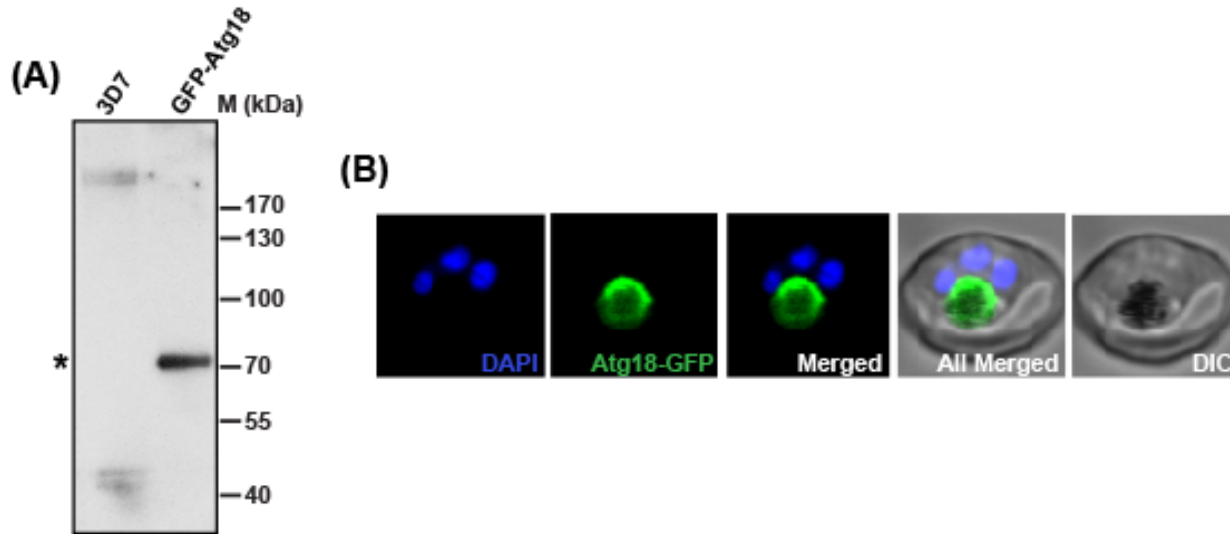
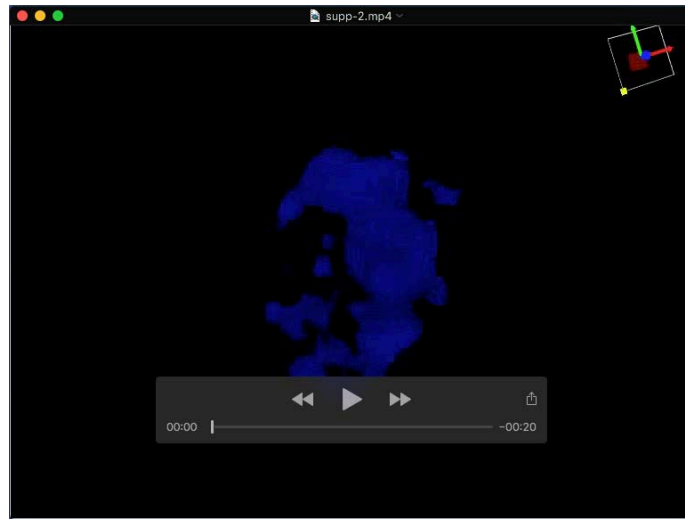
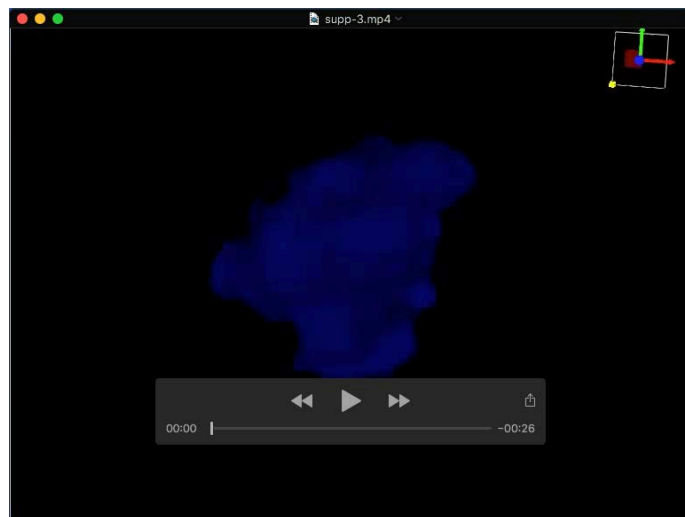


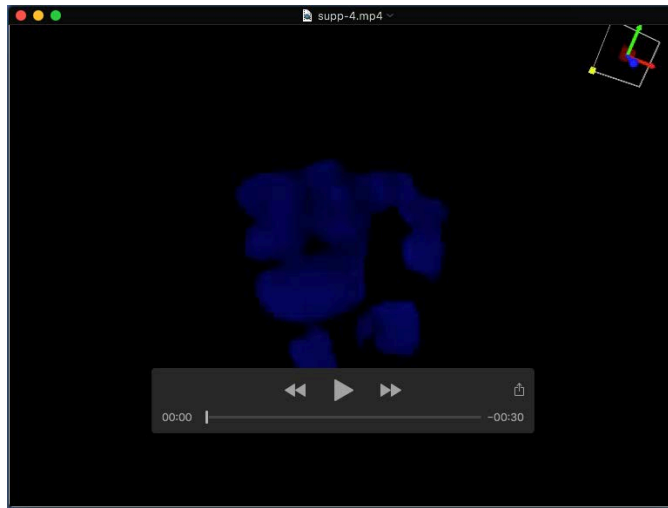
Figure S5. Immunoblotting and live cell imaging to check the expression of GFP-Atg18 in parasites. **(A)** To check the expression of Atg18-GFP in the parasite, lysate were prepared from asynchronous stage 3D7 or Atg18-GFP parasites and resolved in SDS-PAGE followed by Western blotting analysis using antibodies against GFP. “*” indicates the GFP-tagged Atg18 band. No specific band is present in 3D7 un-transfected parasite line. **(B)** Live confocal microscope image showing expression of Atg18-GFP (green) surrounding the food vacuole of the parasite that contains haemozoin. The parasite nuclei were stained with DAPI (blue). All merged panel shows all fluorescence signals including DIC image (containing haemozoin deposition as dark spot).



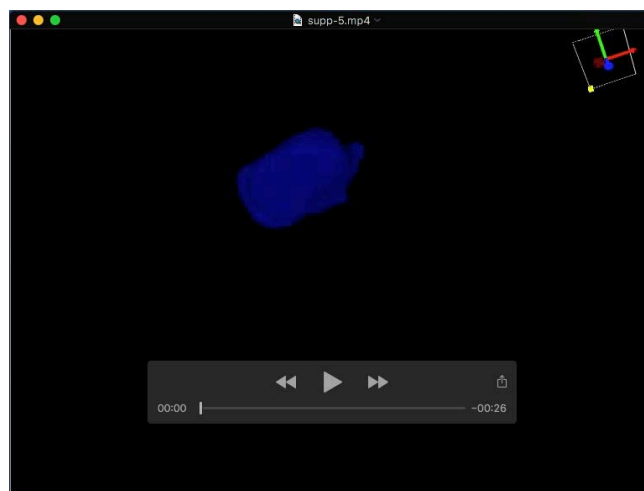
Movie 1: 3D structure of co-localization between PfGCN5 and H3K9Ac in the parasite. Red indicates localization of H3K9Ac and Green indicates localization of PfGCN5. Blue indicates the nuclear region. The movie was generated using Olympus FV31S-SW software.



Movie 2: 3D structure of co-localization between PfGCN5 and PfAtg18-GFP in the DMSO treated parasite. Red indicates localization of PfGCN5 and Green indicates localization of PfAtg18-GFP. Blue indicates the nuclear region. No co-localization was observed in DMSO treated parasite. The movie was generated using Olympus FV31S-SW software.



Movie 3: 3D structure of co-localization between PfGCN5 and PfAtg18-GFP in the MG132 treated parasite. Red indicates localization of PfGCN5 and Green indicates localization of PfAtg18-GFP. Blue indicates the nuclear region. Co-localization was observed between PfGCN5 and PfAtg18-GFP (yellow region). The movie was generated using Olympus FV31S-SW software.



Movie 4: 3D structure of co-localization between PfGCN5 and PfBip in the BFA treated parasite. Red indicates localization of PfBip and Green indicates localization of PfGCN5. Blue indicates the nuclear region. Co-localization was observed between PfGCN5 and PfBip in the ER compartment (yellow region). The movie was generated using Olympus FV31S-SW software.

Table S1: Detailed annotation results generated after PfGCN5 ChIP-sequencing analysis.

[Click here to Download Table S1](#)

Table S2. Primers used in q-PCR analysis

Primers Name	Sequences (5'-3')	Comments
Chr1.(548442-548639)	fw: ATCTATTCTTTTGAATTATGTATA rv: TTCTTTAGAATCCAGCACTT	
Chr2.(838758-838965)	fw: TATCTGTACAATAATTATGTAC rv: ATATTCATCTAACCCTTCAG	
Chr3.(646615-646817)	fw: TAAGTATAAATAAGTTGTTTCATT rv: TTCAACATTCTGAGTAGCC	
Chr4.(319702-319916)	fw: ATAATGTGTATGTATTTATGTAT rv: AATAACAACCTATAATACTAGTAT	
Chr5.(85776-86025)	Fw: AAAGATTTTATCAGGCATTATA rv: TTTATTTATTTATGATTATATATAT	Promoter region for RAP2 (PF3D7_0501600)
Chr6.(545620-545842)	fw: AATAATTTGGTAATTTACTCTT rv: ATATGTATTTGTCTTATTGTTA	Promoter region for RP (PF3D7_0613300)
Chr7.(945701-945935)	fw: ATATATAATTTCTGTGATAAAATAT rv: TTAATAGAATGCTCAATATAAAA	Promoter region for RALP1 (PF3D7_0722200)
Chr9.(1254233-1254434)	fw: AATGAAATAGAAAATATAAAATGA rv: AAGTCCATACAAATTGTAACA	Promoter region for Nop52(PF3D7_0931100)
Chr11.(761384-761633)	fw: ATTATATACATTTGATATAGATAT rv: AATAAATATATAGGTACTIONTAACT	
Control (225279-225528)	fw: ATTATGTATAAGAAGTTCATCA rv: GTATATAAATTCAATGATTTTATA	